

Magnetic Field Effects in the s - d Exchange Model of Dilute Magnetic Alloys

Philip E. Bloomfield* and Robert Hecht†

Physics Department, University of Pennsylvania, ‡ Philadelphia, Pennsylvania 19104

and

Paul R. Sievert

Battelle Memorial Institute, Columbus, Ohio 43201

(Received 2 June 1970)

The effects of arbitrary external magnetic fields on the electronic properties of dilute magnetic alloys are calculated. Two-time thermodynamic Green's-function equations of motion are applied to the s - d exchange model. We generalize Nagaoka's truncation procedure to finite field, conserving total angular momentum, and solve the resulting integral equations using the analytic properties of the Green's functions and a numerical procedure. We calculate the magnetoresistance, magnetization, and the spatial dependence of the conduction-electron spin polarization. The calculations have been performed using values of the model parameters corresponding to a Kondo temperature 16 °K and a CuFe alloy system with an impurity spin of $\frac{1}{2}$ and with equal conduction- and impurity-electron g factors. Our results show a negative magnetoresistance qualitatively in agreement with experiment, but with the field effects somewhat overemphasized. It is found that there is no sizable contribution of the conduction electrons to the susceptibility, which is in agreement with the latest experimental results. Also, the apparent disappearance of the local moment with decreasing temperature is due to an increase in the spin correlation between conduction and impurity electrons, and not due to a spin-compensating electronic cloud forming about the impurity spin. For high temperatures and fields, significant effects of the exchange scattering still persist. There is a nonoscillating component in the conduction-electron spin polarization which damps out in what amounts to 10 lattice spacings for Cu. This is also in agreement with experiment in that no long-range nonoscillatory component has been detected by host NMR studies.

I. INTRODUCTION

Kondo¹ explained the anomalous rise of the low-temperature resistivity of dilute magnetic alloys by calculating in the second Born approximation the correlations which account for the internal degree of freedom of a magnetic impurity scattering center. He used what is called the s - d model which consists of an impurity spin embedded in a Fermi sea of conduction electrons and interacting via the contact-exchange interaction. The second Born approximation yields a logarithmic divergence of the resistivity as the temperature goes to zero which is related to the sharpness of the Fermi surface of the host metal. This nonphysical divergence has been removed by a variety of techniques,² one of which, that of Nagaoka,³ is of particular interest. Nagaoka solved a truncated set of two-time thermodynamic Green's-function equations⁴ whose solution did not contain the divergence but indicated the onset of spin compensation of the impurity spin due to conduction-electron spins condensing around it. Experimentally,⁵ there is an apparent decrease of the local moment as the temperature decreases and this has been interpreted as due to spin compensation. Accompanying the spin compensation, Nagaoka found that a correlation function related to the spatial extent

of the conduction-electron disturbance around the impurity spin contained a negative term of the form $[\sin 2k_F r / r]^2$, where k_F is the Fermi momentum and r is the distance from the impurity site. The indication of a spin-compensated state and the accompanying spin disturbance has stimulated various theories of the ground state and calculations of the spin correlations about the impurity. Fullenbaum and Falk⁶ have calculated and compared various spin-correlation functions using the variational calculation of Appelbaum and Kondo,⁷ Nagaoka's original formulation,³ and the exact solution of Hamann's⁸ formulation of Nagaoka's³ theory by Bloomfield and Hamann.⁹ All of these calculations show a long-range negative definite component in the spatial dependence of these correlation functions of the form first found by Nagaoka.³ Such a disturbance should be seen in the Knight shift of the host metal, and various attempts have been made to interpret experimental data in this fashion.¹⁰ The conduction-electron-local-moment correlation functions calculated, $\langle \vec{s}(r) \cdot \vec{S} \rangle$, have not included an external magnetic field. They are nonzero even in the absence of a field, whereas the true spin polarization, i. e., the number of electrons with spin up minus the number with spin down as a function of r , is nonzero only in an external magnetic field.

A calculation of the spin polarization and magnetic susceptibility in a finite external magnetic field has been done by Heeger *et al.*,¹⁰ based on the Appelbaum-Kondo⁷ variational calculation. NMR and susceptibility measurements in $CuFe$ were also interpreted in these terms by Heeger *et al.*¹⁰ and Golibersuch and Heeger.¹¹ At high temperatures (i. e., greater than T_k , the Kondo temperature) and low field, a calculation of the polarization was done by Fullenbaum and Falk¹² in which they find a modification of the RKKY polarization¹³ at large r . Another perturbation-type calculation was done by Everts and Ganguly¹⁴ who found a result in conflict with Fullenbaum and Falk.¹² There has been a perturbation calculation of the magnetoresistance by Beal-Monod and Weiner¹⁵ which gives a negative magnetoresistance in good agreement with experiment.¹⁶ Also, an S -matrix theory of the magnetoresistance for arbitrary magnetic fields was formulated by More and Suhl¹⁷ with qualitative agreement with experiment. A non-perturbative approach to calculating the susceptibility and true spin polarization in finite magnetic fields was used by Klein.¹⁸ His calculation used two-time thermodynamic Green's function and the truncation scheme of Takano and Ogawa¹⁹ in which the impurity spin operator is broken up into Fermion operators for purposes of truncation. This is in contrast with Nagaoka's³ truncation scheme where they are left intact and total angular momentum is conserved in all thermal averages.

It is our purpose in this paper to calculate the properties of the s - d model in arbitrary external magnetic fields by using two-time thermodynamic Green's functions and to generalize the Nagaoka truncation procedure which conserves total angular momentum. We shall calculate the magnetoresistance, magnetization, and spin polarization, all in a consistent fashion. We shall compare our results with experiment and with the other calculations mentioned above.

Section II contains the theory – the equation of motion, the truncation scheme, the relevant integral equations, and the method of solution. A numerical scheme²⁰ was necessary in this case and the details are given in the Appendix. Also, many of the relevant properties and definitions are in Tables I and II.

Section III contains our results, their comparison with experiment, and their comparison with other calculations. We consider first the magnetoresistivity, then calculate the thermal average of the impurity spin and susceptibility, and finally calculate the spatial dependence of the spin polarization.

In Sec. IV we summarize our results and the conclusions we draw from these calculations.

II. THEORY

Our Hamiltonian is

$$\mathcal{H} = -\gamma g_i S^z + \sum_{\vec{k}\sigma} \epsilon_{\vec{k}\sigma} c_{\vec{k}\sigma}^\dagger c_{\vec{k}\sigma} - \frac{J}{2N} \sum_{\vec{k}\vec{k}'\sigma} (\sigma c_{\vec{k}\sigma}^\dagger c_{\vec{k}'\sigma} S^z + c_{\vec{k}\sigma}^\dagger c_{\vec{k}'\sigma} S^y), \quad (1)$$

where $\sigma = -\bar{\sigma} = \pm 1$ or \uparrow, \downarrow corresponding to spin up or down, respectively; $\epsilon_{\vec{k}\sigma} = \epsilon_{\vec{k}} - \sigma g_e \gamma / 2$, where $\epsilon_{\vec{k}}$ is the single-particle energy with the zero of energy being the Fermi energy; $\gamma = \mu_B H$, where μ_B is the Bohr magneton and H is the magnitude of the external magnetic field which is taken to be pointing opposite the z axis. We take g_e and g_i , the electron- and impurity-spin g factors, to be positive so that the lower energy is associated with the spins up. For electrons, $\mathcal{H}_{\text{Mag}} = |g| \mu_B \vec{S} \cdot \vec{H}$ and Eq. (1) shows that spin up [positive $\langle S^z \rangle$ or S_e from Eq. (65) below] corresponds to spins antiparallel to \vec{H} having the lower energy. The $c_{\vec{k}\sigma}^\dagger$ and $c_{\vec{k}\sigma}$ are conduction-electron creation and annihilation operators on states \vec{k} and σ , respectively, and the impurity spin operator is \vec{S} , such that $S^z = S^x \pm i S^y$. J is the s - d coupling constant and N is the number of unit cells in the lattice.

By using the method of double-time thermodynamic Green's functions⁴ we have for the equation of motion of the single-particle function $\mathcal{G}_{\vec{k}\vec{k}'}^\sigma$,

$$i \frac{\partial}{\partial t} \mathcal{G}_{\vec{k}\vec{k}'}^\sigma = \delta_{\vec{k}\vec{k}'} \delta(t) + \epsilon_{\vec{k}'\sigma} \mathcal{G}_{\vec{k}\vec{k}'}^\sigma - \frac{J}{2N} \sum_{\vec{l}} (\mathcal{P}_{\vec{k}\vec{l}}^\sigma + \mathcal{S}_{\vec{k}\vec{l}}^\sigma). \quad (2)$$

The Green's function and various thermal averages that are used are defined in Table I. The double-angular-bracket notation in Table I corresponds to the usual definition⁴ of retarded Green's functions, i. e., in terms of operators A and B ,

$$\langle\langle A | B \rangle\rangle = -i\theta(t) \langle [A(t), B(0)]_+ \rangle, \quad (3)$$

where the single angular bracket denotes statistical average, the $+$ denotes an anticommutator, and $\theta(t)$ is a step function. The equation of motion for the $\mathcal{P}_{\vec{k}\vec{k}'}^\sigma$ and $\mathcal{S}_{\vec{k}\vec{k}'}^\sigma$ are

$$i \frac{\partial}{\partial t} \mathcal{P}_{\vec{k}\vec{k}'}^\sigma = \sigma \langle S^z \rangle \delta_{\vec{k}\vec{k}'} \delta(t) + \epsilon_{\vec{k}'\sigma} \mathcal{P}_{\vec{k}\vec{k}'}^\sigma - \frac{J}{2N} \sum_{\vec{l}} \langle\langle (S^z)^2 c_{\vec{l}\sigma} | c_{\vec{k}\sigma}^\dagger \rangle\rangle - \frac{J}{2N} \sigma \sum_{\vec{l}} \langle\langle S^z S^y c_{\vec{l}\sigma} | c_{\vec{k}\sigma}^\dagger \rangle\rangle + \frac{J}{2N} \sigma \sum_{\vec{l}\vec{l}'\sigma'} \langle\langle S^y c_{\vec{l}\sigma'}^\dagger c_{\vec{l}'\sigma} c_{\vec{k}\sigma} | c_{\vec{k}\sigma}^\dagger \rangle\rangle \quad (4)$$

and

$$i \frac{\partial}{\partial t} \mathcal{S}_{\vec{k}\vec{k}'}^\sigma = (\epsilon_{\vec{k}'\sigma} - \sigma \gamma g_i) \mathcal{S}_{\vec{k}\vec{k}'}^\sigma + \frac{J}{2N} \sum_{\vec{l}} \langle\langle \sigma S^y S^z c_{\vec{l}\sigma} - S^y S^z c_{\vec{l}\sigma} | c_{\vec{k}\sigma}^\dagger \rangle\rangle$$

$$+ \frac{J}{2N} \sum_{\vec{k}} \langle \langle (S^{\vec{\sigma}} c_{\vec{k}\vec{\sigma}}^{\dagger} c_{\vec{k}\vec{\sigma}} - c_{\vec{k}\vec{\sigma}}^{\dagger} c_{\vec{k}\vec{\sigma}}) + 2\sigma S^{\vec{\sigma}} c_{\vec{k}\vec{\sigma}}^{\dagger} c_{\vec{k}\vec{\sigma}} \rangle \rangle c_{\vec{k}\vec{\sigma}}^{\dagger} | c_{\vec{k}\vec{\sigma}}^{\dagger} \rangle \rangle. \quad (5)$$

We truncate the chain of equations by factoring the higher-order Green's functions which appear on the right-hand side of Eqs. (4) and (5). In order to do this we use the cumulant expansion technique.²¹ We set the cumulant Green's function corresponding to our retarded Green's function equal to zero. Thus, we neglect statistically linked higher-order correlations and thereby obtain an expansion for our higher-order Green's functions in terms of those of lower-order and certain time-independent thermal averages. Those thermal averages obtained that do not conserve particle number or angular momentum are set equal to zero. Since the Hamiltonian conserves particle number and angular momentum, we know that in an exact treatment these averages must be zero. Furthermore, in addition to the sign attached to each term by the conventions of the cumulant expansion,²² we attach an additional sign $(-1)^n$, where n is the number of interchanges of creation or annihilation operators necessary to bring the factored function into the same ordered form as the unfactored function. Carrying out this procedure the four higher-order Green's functions needed are approximated as

$$\langle \langle S^{\vec{\sigma}} c_{\vec{k}\vec{\sigma}}^{\dagger} c_{\vec{k}\vec{\sigma}} c_{\vec{k}\vec{\sigma}}^{\dagger} | c_{\vec{k}\vec{\sigma}}^{\dagger} \rangle \rangle \approx \langle S^{\vec{\sigma}} c_{\vec{k}\vec{\sigma}}^{\dagger} c_{\vec{k}\vec{\sigma}} \rangle \mathcal{G}_{\vec{k}\vec{\sigma}}^{\vec{\sigma}}, \\ - \delta_{\sigma\sigma'} \langle c_{\vec{k}\vec{\sigma}}^{\dagger} c_{\vec{k}\vec{\sigma}'} \rangle \mathcal{G}_{\vec{k}\vec{\sigma}}^{\vec{\sigma}} - \delta_{\sigma\sigma'} \langle S^{\vec{\sigma}} c_{\vec{k}\vec{\sigma}}^{\dagger} c_{\vec{k}\vec{\sigma}'} \rangle \mathcal{G}_{\vec{k}\vec{\sigma}}^{\vec{\sigma}}, \quad (6a)$$

$$\langle \langle S^{\vec{\sigma}} c_{\vec{k}\vec{\sigma}}^{\dagger} c_{\vec{k}\vec{\sigma}} c_{\vec{k}\vec{\sigma}}^{\dagger} | c_{\vec{k}\vec{\sigma}}^{\dagger} \rangle \rangle \approx \langle c_{\vec{k}\vec{\sigma}}^{\dagger} c_{\vec{k}\vec{\sigma}} \rangle \mathcal{G}_{\vec{k}\vec{\sigma}}^{\vec{\sigma}} - \langle c_{\vec{k}\vec{\sigma}}^{\dagger} c_{\vec{k}\vec{\sigma}} \rangle \mathcal{G}_{\vec{k}\vec{\sigma}}^{\vec{\sigma}}, \quad (6b)$$

$$\langle \langle S^{\vec{\sigma}} c_{\vec{k}\vec{\sigma}}^{\dagger} c_{\vec{k}\vec{\sigma}} c_{\vec{k}\vec{\sigma}}^{\dagger} | c_{\vec{k}\vec{\sigma}}^{\dagger} \rangle \rangle \approx \langle c_{\vec{k}\vec{\sigma}}^{\dagger} c_{\vec{k}\vec{\sigma}} \rangle \mathcal{G}_{\vec{k}\vec{\sigma}}^{\vec{\sigma}} - \langle S^{\vec{\sigma}} c_{\vec{k}\vec{\sigma}}^{\dagger} c_{\vec{k}\vec{\sigma}} \rangle \mathcal{G}_{\vec{k}\vec{\sigma}}^{\vec{\sigma}}, \quad (6c)$$

and

$$\langle \langle S^{\vec{\sigma}} c_{\vec{k}\vec{\sigma}}^{\dagger} c_{\vec{k}\vec{\sigma}} c_{\vec{k}\vec{\sigma}}^{\dagger} | c_{\vec{k}\vec{\sigma}}^{\dagger} \rangle \rangle \approx - \langle c_{\vec{k}\vec{\sigma}}^{\dagger} c_{\vec{k}\vec{\sigma}} \rangle \mathcal{P}_{\vec{k}\vec{\sigma}}^{\vec{\sigma}} - \langle S^{\vec{\sigma}} c_{\vec{k}\vec{\sigma}}^{\dagger} c_{\vec{k}\vec{\sigma}} \rangle \mathcal{G}_{\vec{k}\vec{\sigma}}^{\vec{\sigma}} \\ + 2 \langle S^{\vec{\sigma}} \rangle \langle c_{\vec{k}\vec{\sigma}}^{\dagger} c_{\vec{k}\vec{\sigma}} \rangle \mathcal{G}_{\vec{k}\vec{\sigma}}^{\vec{\sigma}} + \langle S^{\vec{\sigma}} \rangle \langle \langle c_{\vec{k}\vec{\sigma}}^{\dagger} c_{\vec{k}\vec{\sigma}} c_{\vec{k}\vec{\sigma}}^{\dagger} | c_{\vec{k}\vec{\sigma}}^{\dagger} \rangle \rangle. \quad (6d)$$

Finally, the last term on the right-hand side of

TABLE I. Green's functions and thermal averages defined for finite external magnetic field.

$\mathcal{G}_{\vec{k}\vec{\sigma}}^{\vec{\sigma}} \equiv \langle \langle c_{\vec{k}\vec{\sigma}}^{\dagger} c_{\vec{k}\vec{\sigma}} \rangle \rangle$	$\mathcal{G}_{\vec{k}}^{\vec{\sigma}} \equiv \sum_{\vec{k}} \mathcal{G}_{\vec{k}\vec{\sigma}}^{\vec{\sigma}}$
$\mathcal{E}_{\vec{k}\vec{\sigma}}^{\vec{\sigma}} \equiv \langle \langle S^{\vec{\sigma}} c_{\vec{k}\vec{\sigma}}^{\dagger} c_{\vec{k}\vec{\sigma}} \rangle \rangle$	$\mathcal{E}_{\vec{k}}^{\vec{\sigma}} \equiv \sum_{\vec{k}} \mathcal{E}_{\vec{k}\vec{\sigma}}^{\vec{\sigma}}$
$\mathcal{P}_{\vec{k}\vec{\sigma}}^{\vec{\sigma}} \equiv \langle \langle S^{\vec{\sigma}} c_{\vec{k}\vec{\sigma}}^{\dagger} c_{\vec{k}\vec{\sigma}} \rangle \rangle$	$\mathcal{P}_{\vec{k}}^{\vec{\sigma}} \equiv \sum_{\vec{k}} \mathcal{P}_{\vec{k}\vec{\sigma}}^{\vec{\sigma}}$
$n_{\vec{k}\vec{\sigma}}^{\vec{\sigma}} \equiv \sum_{\vec{k}} \langle c_{\vec{k}\vec{\sigma}}^{\dagger} c_{\vec{k}\vec{\sigma}} \rangle$	$\Delta \equiv \sum_{\vec{k}} (n_{\vec{k}\vec{\sigma}}^{\vec{\sigma}} - n_{\vec{k}\vec{\sigma}}^{\vec{\sigma}'})$
$L_{\vec{k}\vec{\sigma}}^{\vec{\sigma}} \equiv \sum_{\vec{k}} \langle c_{\vec{k}\vec{\sigma}}^{\dagger} c_{\vec{k}\vec{\sigma}} c_{\vec{k}\vec{\sigma}}^{\dagger} S^{\vec{\sigma}} \rangle$	
$M_{\vec{k}\vec{\sigma}}^{\vec{\sigma}} \equiv 2 \sum_{\vec{k}} \langle c_{\vec{k}\vec{\sigma}}^{\dagger} c_{\vec{k}\vec{\sigma}} c_{\vec{k}\vec{\sigma}}^{\dagger} S^{\vec{\sigma}} \rangle$	

Eq. (6d) is approximated as

$$\langle \langle c_{\vec{k}\vec{\sigma}}^{\dagger} c_{\vec{k}\vec{\sigma}} c_{\vec{k}\vec{\sigma}}^{\dagger} | c_{\vec{k}\vec{\sigma}}^{\dagger} \rangle \rangle \approx - \langle c_{\vec{k}\vec{\sigma}}^{\dagger} c_{\vec{k}\vec{\sigma}} \rangle \mathcal{G}_{\vec{k}\vec{\sigma}}^{\vec{\sigma}}. \quad (6e)$$

Note that when the external magnetic field is zero, $\langle S^{\vec{\sigma}} \rangle = 0$ and up-down symmetry can be invoked to reduce the above approximation scheme to that of Nagaoka.³ For simplicity, we now specialize our treatment to the case of impurity spin $\frac{1}{2}$ for which

$$(S^{\vec{\sigma}})^2 = \frac{1}{4}, \quad S^{\vec{\sigma}} S^{\vec{\sigma}'} = -S^{\vec{\sigma}'} S^{\vec{\sigma}} = \vec{\sigma} S^{\vec{\sigma}'} / 2, \quad (7)$$

and

$$S^{\vec{\sigma}} S^{\vec{\sigma}'} = \frac{1}{2} + \vec{\sigma} S^{\vec{\sigma}'}.$$

Inserting Eqs. (6) and (7) into (4) and (5) and using the thermal averages and Green's functions defined in Table I we obtain

$$i \frac{\partial}{\partial t} \mathcal{P}_{\vec{k}\vec{\sigma}}^{\vec{\sigma}} = \sigma \langle S^{\vec{\sigma}} \rangle \delta_{\vec{k}\vec{\sigma}} \delta(t) + \epsilon_{\vec{k}\vec{\sigma}} \mathcal{P}_{\vec{k}\vec{\sigma}}^{\vec{\sigma}} \\ + \frac{J}{2N} (L_{\vec{k}\vec{\sigma}}^{\vec{\sigma}} - \frac{1}{4}) \mathcal{G}_{\vec{k}}^{\vec{\sigma}} - \frac{J}{2N} (n_{\vec{k}\vec{\sigma}}^{\vec{\sigma}} - \frac{1}{2}) \mathcal{E}_{\vec{k}}^{\vec{\sigma}} \\ - \sigma \frac{J}{2N} \mathcal{G}_{\vec{k}\vec{\sigma}}^{\vec{\sigma}} \sum_{\vec{\sigma}'} \sigma' L_{\vec{k}\vec{\sigma}'}^{\vec{\sigma}'}, \quad (8)$$

and

$$i \frac{\partial}{\partial t} \mathcal{E}_{\vec{k}\vec{\sigma}}^{\vec{\sigma}} = \left(\epsilon_{\vec{k}\vec{\sigma}} - \sigma \gamma g_i - \frac{J}{2N} \sigma \Delta \right) \mathcal{E}_{\vec{k}\vec{\sigma}}^{\vec{\sigma}} \\ - \frac{J}{2N} (n_{\vec{k}\vec{\sigma}}^{\vec{\sigma}} - \frac{1}{2}) (\mathcal{E}_{\vec{k}}^{\vec{\sigma}} + 2\mathcal{P}_{\vec{k}}^{\vec{\sigma}}) \\ + \frac{J}{2N} \left(-\frac{1}{2} + L_{\vec{k}\vec{\sigma}}^{\vec{\sigma}} - \sigma M_{\vec{k}\vec{\sigma}}^{\vec{\sigma}} + 2\sigma \langle S_{\vec{z}} \rangle n_{\vec{k}\vec{\sigma}}^{\vec{\sigma}} \right) \mathcal{G}_{\vec{k}}^{\vec{\sigma}}. \quad (9)$$

Note that the energy shift $J\sigma\Delta/2N$ in Eq. (9) is expressible in terms of the net conduction-electron spin density on the impurity site [see Eq. (70) and Sec. III C]. The last term on the right-hand side of Eq. (8) is equal to zero, viz.,

$$\Lambda \equiv \sum_{\vec{\sigma}} (L_{\vec{\sigma}} - L_{\vec{\sigma}'}) = 0. \quad (10)$$

To show this, we consider

$$\frac{\partial}{\partial t} S^{\vec{\sigma}} = i [\mathcal{H}, S^{\vec{\sigma}}] = -i \frac{J}{2N} \sum_{\vec{k}} (c_{\vec{k}\vec{\sigma}}^{\dagger} c_{\vec{k}\vec{\sigma}} S^{\vec{\sigma}} - c_{\vec{k}\vec{\sigma}}^{\dagger} c_{\vec{k}\vec{\sigma}} S^{\vec{\sigma}'}) \quad (11)$$

and take the statistical average to obtain

$$\left\langle \frac{\partial}{\partial t} S^{\vec{\sigma}} \right\rangle = i \frac{J}{2N} \Lambda. \quad (12)$$

Since $\langle \partial S^{\vec{\sigma}} / \partial t \rangle = \partial \langle S^{\vec{\sigma}} \rangle / \partial t$ and $\langle S^{\vec{\sigma}} \rangle$ is independent of time, we have $\Lambda = 0$.

Now we introduce the Fourier transforms

$$\mathcal{G}(\omega) = (2\pi)^{-1} \int_{-\infty}^{\infty} dt e^{i\omega t} \mathcal{G}(t), \quad (13) \\ \mathcal{G}_{\vec{k}\vec{\sigma}}^{\vec{\sigma}}(\omega) = (\omega - \epsilon_{\vec{k}\vec{\sigma}})^{-1} \{ \delta_{\vec{k}\vec{\sigma}} / 2\pi - (J/2N) [\mathcal{P}_{\vec{k}}^{\vec{\sigma}}(\omega) + \mathcal{E}_{\vec{k}}^{\vec{\sigma}}(\omega)] \}, \quad (14a)$$

$$\mathcal{P}_{\vec{k}\vec{\sigma}}^{\vec{\sigma}}(\omega) = (\omega - \epsilon_{\vec{k}\vec{\sigma}})^{-1} [\sigma \langle S^{\vec{\sigma}} \rangle \delta_{\vec{k}\vec{\sigma}} / 2\pi \\ + (J/2N) (L_{\vec{k}\vec{\sigma}}^{\vec{\sigma}} - \frac{1}{4}) \mathcal{G}_{\vec{k}}^{\vec{\sigma}}(\omega) - (J/2N) (n_{\vec{k}\vec{\sigma}}^{\vec{\sigma}} - \frac{1}{2}) \mathcal{E}_{\vec{k}}^{\vec{\sigma}}(\omega)], \quad (14b)$$

TABLE II. Fundamental functions and their symmetry properties for finite external magnetic fields; z is the complex energy.

$F^\sigma(z) \equiv \sum_{\mathbf{k}} \tilde{f}(z - \epsilon_{\mathbf{k}\sigma}^*)^{-1}$	
$g_1^\sigma(z) \equiv \sum_{\mathbf{k}} \tilde{f}[\epsilon_{\mathbf{k}\sigma}^* - \frac{1}{2}] (z - \epsilon_{\mathbf{k}\sigma}^*)^{-1}$	
$f(\epsilon_{\mathbf{k}\sigma}^*)$ is the Fermi distribution function.	
$G_1^\sigma(z) \equiv \sum_{\mathbf{k}} \tilde{f}(n_{\mathbf{k}\sigma}^* - \frac{1}{2}) (z - \epsilon_{\mathbf{k}\sigma}^*)^{-1}$	
$G_2^\sigma(z) \equiv \sum_{\mathbf{k}} \tilde{f}(n_{\mathbf{k}\sigma}^* - \frac{1}{2}) [z - \epsilon_{\mathbf{k}\sigma}^* + \sigma g_i \gamma + (J/2N)\sigma\Delta]^{-1}$	
$= G_1^\sigma(z + \sigma g_i \gamma + (J/2N)\sigma\Delta)$	
$E^\sigma(z) \equiv \sum_{\mathbf{k}} \tilde{f}(\frac{1}{2} - L_{\mathbf{k}\sigma}^*) (z - \epsilon_{\mathbf{k}\sigma}^*)^{-1}$	
$P^\sigma(z)$	
$\equiv \sum_{\mathbf{k}} \tilde{f}(\frac{1}{2} - L_{\mathbf{k}\sigma}^* + \sigma M_{\mathbf{k}\sigma}^* - 2\sigma \langle S^z \rangle n_{\mathbf{k}\sigma}^*) [z - \epsilon_{\mathbf{k}\sigma}^* + \sigma g_i \gamma (J/2N)\sigma\Delta]^{-1}$	
Reality condition	Particle-hole symmetry
$[F^\sigma(z^*)]^* = F^\sigma(z)$	$-F^\sigma(-z) = F^\sigma(z)$
$[g^\sigma(z^*)]^* = g^\sigma(z)$	$g^\sigma(-z) = g^\sigma(z)$
$[G_1^\sigma(z^*)]^* = G_1^\sigma(z)$	$G_1^\sigma(-z) = G_1^\sigma(z)$
$[G_2^\sigma(z^*)]^* = G_2^\sigma(z)$	$G_2^\sigma(-z) = G_2^\sigma(z)$
$[E^\sigma(z^*)]^* = E^\sigma(z)$	$-E^\sigma(-z) = E^\sigma(z)$
$[P^\sigma(z^*)]^* = P^\sigma(z)$	$-P^\sigma(-z) = P^\sigma(z)$
$[t_{G,E}^\sigma(z^*)]^* = t_{G,E}^\sigma(z)$	$-t_{G,E}^\sigma(-z) = t_{G,E}^\sigma(z)$
$[\varphi_G^\sigma(z^*)]^* = \varphi_G^\sigma(z)$	$\varphi_G^\sigma(-z) = \varphi_G^\sigma(z)$
$[\Phi_{G,E}^\sigma(z^*)]^* = \Phi_{G,E}^\sigma(z)$	$-\Phi_{G,E}^\sigma(-z) = \Phi_{G,E}^\sigma(z)$

and

$$\begin{aligned} \delta_{\mathbf{k}\sigma}^\sigma(\omega) &= (\omega - \epsilon_{\mathbf{k}\sigma}^* + \sigma \gamma g_i + \sigma \Delta J/2N)^{-1} \\ &\times \left\{ - (J/2N) \left(\frac{1}{2} - L_{\mathbf{k}\sigma}^* + \sigma M_{\mathbf{k}\sigma}^* - 2\sigma \langle S^z \rangle n_{\mathbf{k}\sigma}^* \right) \mathcal{G}_{\mathbf{k}\sigma}^\sigma(\omega) \right. \\ &\left. - (J/2N) \left(n_{\mathbf{k}\sigma}^* - \frac{1}{2} \right) [\delta_{\mathbf{k}\sigma}^\sigma(\omega) + 2\mathcal{O}_{\mathbf{k}\sigma}^\sigma(\omega)] \right\}. \quad (14c) \end{aligned}$$

Note that since we are using retarded Green's functions, unless explicitly stated ω is taken just above the real axis, i. e., $\omega + i\delta$ on the complex-energy plane. Summing Eqs. (14) over \mathbf{k}' and referring to the definitions in Table I, we can solve for $\mathcal{G}_{\mathbf{k}\sigma}^\sigma$, $\mathcal{O}_{\mathbf{k}\sigma}^\sigma$, and $\mathcal{P}_{\mathbf{k}\sigma}^\sigma$ in terms of two "t matrices," viz.,

$$2\pi \mathcal{G}_{\mathbf{k}\sigma}^\sigma(\omega) = (\omega - \epsilon_{\mathbf{k}\sigma}^*)^{-1} [1 + F^\sigma(\omega) t_G^\sigma(\omega)], \quad (15a)$$

$$-2\pi (J/2N) \delta_{\mathbf{k}\sigma}^\sigma(\omega) = (\omega - \epsilon_{\mathbf{k}\sigma}^*)^{-1} t_E^\sigma(\omega), \quad (15b)$$

and

$$-2\pi (J/2N) \mathcal{P}_{\mathbf{k}\sigma}^\sigma(\omega) = (\omega - \epsilon_{\mathbf{k}\sigma}^*)^{-1} [t_G^\sigma(\omega) - t_E^\sigma(\omega)], \quad (15c)$$

where in terms of the definitions of $F^\sigma(\omega)$, $G_1^\sigma(\omega)$, $G_2^\sigma(\omega)$, $E^\sigma(\omega)$, and $P^\sigma(\omega)$ given in Table II we have

$$t_G^\sigma(\omega) = -\frac{J}{2N} [A^\sigma(\omega)]^{-1} \left[\left(1 - \frac{J}{2N} G_2^\sigma(\omega) \right) \left(\sigma \langle S^z \rangle - \frac{J}{2N} E^\sigma(\omega) \right) \right.$$

$$\left. - \frac{J}{2N} P^\sigma(\omega) \left(1 - \frac{J}{2N} G_1^\sigma(\omega) \right) \right] \quad (16a)$$

and

$$\begin{aligned} t_E^\sigma(\omega) &= \left(\frac{J}{2N} \right)^2 [A^\sigma(\omega)]^{-1} \left[2G_2^\sigma(\omega) \left(\sigma \langle S^z \rangle - \frac{J}{2N} E^\sigma(\omega) \right) \right. \\ &\left. + P^\sigma(\omega) \left(1 - \frac{J}{2N} \sigma \langle S^z \rangle F^\sigma(\omega) \right) \right], \quad (16b) \end{aligned}$$

where

$$\begin{aligned} A^\sigma(\omega) &= \left(1 - \frac{J}{2N} G_2^\sigma(\omega) \right) \left[1 - \left(\frac{J}{2N} \right)^2 F^\sigma(\omega) E^\sigma(\omega) \right] \\ &+ \frac{J}{2N} \left(1 - \frac{J}{2N} G_1^\sigma(\omega) \right) \left(2G_2^\sigma(\omega) - \frac{J}{2N} F^\sigma(\omega) P^\sigma(\omega) \right). \quad (16c) \end{aligned}$$

In order to proceed we need to obtain expressions for the correlation functions used in these definitions. All correlation functions which arise in the truncation process can be written in terms of $t_G^\sigma(\omega)$ and $t_E^\sigma(\omega)$ by using Eqs. (15) and the relation⁴

$$\langle BA \rangle = i \int_{-\infty}^{\infty} d\omega f(\omega) (\langle \langle A|B \rangle \rangle_{\omega+i\delta} - \langle \langle A|B \rangle \rangle_{\omega-i\delta}), \quad (17)$$

where $f(\omega)$ is the Fermi distribution function.

Hence, using the definitions given in Table I and the identity⁴

$$\langle \langle A, B \rangle \rangle_+ = i \int_{-\infty}^{\infty} d\omega (\langle \langle A|B \rangle \rangle_{\omega+i\delta} - \langle \langle A|B \rangle \rangle_{\omega-i\delta}), \quad (18)$$

we obtain [using the Plemlj relation of Eq. (35) below]

$$\begin{aligned} n_{\mathbf{k}\sigma}^* &= \sum_{\mathbf{k}'} \langle c_{\mathbf{k}\sigma}^\dagger c_{\mathbf{k}'\sigma} \rangle \\ &= i \int_{-\infty}^{\infty} d\omega [f(\omega) - \frac{1}{2}] [\mathcal{G}_{\mathbf{k}\sigma}^\sigma(\omega + i\delta) - \mathcal{G}_{\mathbf{k}\sigma}^\sigma(\omega - i\delta)] + \frac{1}{2}, \quad (19a) \end{aligned}$$

$$\begin{aligned} L_{\mathbf{k}\sigma} &= \sum_{\mathbf{k}'} \langle S^z c_{\mathbf{k}\sigma}^\dagger c_{\mathbf{k}'\sigma} \rangle \\ &= i \int_{-\infty}^{\infty} d\omega [f(\omega) - \frac{1}{2}] [\mathcal{O}_{\mathbf{k}\sigma}^\sigma(\omega + i\delta) - \mathcal{O}_{\mathbf{k}\sigma}^\sigma(\omega - i\delta)], \quad (19b) \end{aligned}$$

and

$$\begin{aligned} \sigma M_{\mathbf{k}\sigma}^* &= 2\sigma \sum_{\mathbf{k}'} \langle S^z c_{\mathbf{k}\sigma}^\dagger c_{\mathbf{k}'\sigma} \rangle \\ &= i \int_{-\infty}^{\infty} d\omega [f(\omega) - \frac{1}{2}] [\mathcal{P}_{\mathbf{k}\sigma}^\sigma(\omega + i\delta) - \mathcal{P}_{\mathbf{k}\sigma}^\sigma(\omega - i\delta)] \\ &+ \frac{1}{2} \sigma \langle S^z \rangle. \quad (19c) \end{aligned}$$

We have used the fact that $\langle S^z \rangle = 0$. Also we have used the form $[f(\omega) - \frac{1}{2}]$ because it is of definite symmetry, i. e., odd in ω . Note that from the spectral representation of $\mathcal{G}_{\mathbf{k}\sigma}^\sigma$ we find

$$[\mathcal{G}_{\mathbf{k}\sigma}^\sigma(\omega - i\delta)]^* = \mathcal{G}_{\mathbf{k}\sigma}^\sigma(\omega + i\delta), \quad (20)$$

which implies that

$$t_G^\sigma(\omega + i\delta) = t_G^{\sigma*}(\omega - i\delta) \quad (21)$$

and, hence, that $n_{\mathbf{k}\sigma}$ is real. By assuming the same relation holds for t_E^σ we are lead to the reality of $L_{\mathbf{k}\sigma}$ and $M_{\mathbf{k}\sigma}$, as well as $n_{\mathbf{k}\sigma}$ (see the definitions of the thermal averages in terms of the spectral representation above). From the definitions in Table II and by Eq. (17) we see that this assumption is self-consistent with Eq. (16). We call the symmetry condition of Eqs. (20) and (21) the reality condition. We must next find an expression for $\langle S^z \rangle$ in terms of $t_G^\sigma(\omega)$ and $t_E^\sigma(\omega)$.

In order to calculate $\langle S^z \rangle$ we define

$$s^+ = \sum_{\mathbf{k}} c_{\mathbf{k}}^\dagger c_{\mathbf{k}}, \quad (22)$$

and calculate the equation of motion for the Green's function

$$\mathfrak{D}(t) \equiv \langle\langle S^+ + s^+ | S^- \rangle\rangle. \quad (23)$$

We obtain

$$i \frac{\partial \mathfrak{D}}{\partial t} = (1 + 2\langle s^+ S^- \rangle) \delta(t) + \gamma g_i \langle\langle S^+ | S^- \rangle\rangle + \gamma g_e \langle\langle s^+ | S^- \rangle\rangle. \quad (24)$$

At this point, we specialize our calculation to the case of equal g factors, i. e., $g_e = g_i = g$ in order to obtain a closed expression for $\langle S^z \rangle$. After Fourier transforming Eq. (24) we obtain

$$\mathfrak{D}(\omega) = (1 + 2\langle s^+ S^- \rangle) [2\pi(\omega - \gamma g)]^{-1}. \quad (25)$$

Using Eqs. (7), (17), and (25) we find

$$\begin{aligned} \langle S^- S^+ + S^- s^+ \rangle &= \frac{1}{2} - \langle S^z \rangle + \langle s^+ S^- \rangle \\ &= i \int_{-\infty}^{\infty} d\omega f(\omega) [\mathfrak{D}(\omega + i\delta) - \mathfrak{D}(\omega - i\delta)] \\ &= (1 + 2\langle s^+ S^- \rangle) f(\gamma g) \end{aligned} \quad (26)$$

and hence the exact expression

$$\langle S^z \rangle = \left(\frac{1}{2} + \langle s^+ S^- \rangle\right) \tanh(\gamma g / 2kT). \quad (27)$$

Now from the definition of the Green's function $\mathcal{G}_{\mathbf{k}\mathbf{k}'}^\sigma$ in Table I and Eqs. (16) and (17) we have

$$\langle s^+ S^- \rangle = \sum_{\mathbf{k}} i \int_{-\infty}^{\infty} d\omega [f(\omega) - \frac{1}{2}] [\mathcal{G}_{\mathbf{k}\mathbf{k}}^\dagger(\omega + i\delta) - \mathcal{G}_{\mathbf{k}\mathbf{k}}^\dagger(\omega - i\delta)]. \quad (28)$$

Using Eqs. (14c) and (15) we obtain

$$\begin{aligned} \sum_{\mathbf{k}} \mathcal{G}_{\mathbf{k}\mathbf{k}}^\sigma &= \frac{-1}{2\pi} \frac{J}{2N} \\ &\times \sum_{\mathbf{k}} \frac{[\frac{1}{2} - L_{\mathbf{k}\sigma} + \sigma M_{\mathbf{k}\sigma} - 2\sigma \langle S^z \rangle n_{\mathbf{k}\sigma}] [1 + F^\sigma(\omega) t_G^\sigma(\omega)]}{(\omega - \epsilon_{\mathbf{k}\sigma})(\omega - \epsilon_{\mathbf{k}\sigma} + \sigma \gamma g_i + \sigma \Delta J / 2N)} \\ &+ \frac{1}{2\pi} \sum_{\mathbf{k}} \frac{(n_{\mathbf{k}\sigma} - \frac{1}{2}) [2t_G^\sigma(\omega) - t_E^\sigma(\omega)]}{(\omega - \epsilon_{\mathbf{k}\sigma})(\omega - \epsilon_{\mathbf{k}\sigma} + \sigma \gamma g_i + \sigma \Delta J / 2N)}. \end{aligned} \quad (29)$$

For the case of equal g factors, i. e., $g_e = g_i = g$, we can use the partial fraction expansion

$$\begin{aligned} &\left[(\omega - \epsilon_{\mathbf{k}\sigma}) \left(\omega - \epsilon_{\mathbf{k}\sigma} + \sigma \gamma g + \sigma \Delta \frac{J}{2N} \right) \right]^{-1} \\ &= \left(\frac{J}{2N} \Delta \right)^{-1} \left[(\omega - \epsilon_{\mathbf{k}\sigma})^{-1} - \left(\omega - \epsilon_{\mathbf{k}\sigma} + \sigma \frac{J}{2N} \Delta \right)^{-1} \right] \end{aligned} \quad (30)$$

and the definitions given in Table II to express

$$\sum_{\mathbf{k}} \frac{(n_{\mathbf{k}\sigma} - \frac{1}{2})}{(\omega - \epsilon_{\mathbf{k}\sigma})} = G_2^\sigma \left(\omega - \sigma \frac{J}{2N} \Delta \right) = G_1^\sigma(\omega + \sigma g \gamma), \quad (31a)$$

$$\sum_{\mathbf{k}} \frac{(\frac{1}{2} - L_{\mathbf{k}\sigma} + \sigma M_{\mathbf{k}\sigma} - 2\sigma \langle S^z \rangle n_{\mathbf{k}\sigma})}{(\omega - \epsilon_{\mathbf{k}\sigma})} = P^\sigma \left(\omega - \sigma \frac{J}{2N} \Delta \right). \quad (31b)$$

By definition, to go from $G_1^\sigma(\omega)$ to $G_1^\sigma(\omega + \sigma g \gamma)$ we first reverse the sign of the spin and then shift the frequency $\omega \rightarrow \omega + \sigma g \gamma$. In these terms we finally obtain

$$\begin{aligned} 2\pi\sigma \frac{J}{2N} \Delta \sum_{\mathbf{k}} \mathcal{G}_{\mathbf{k}\mathbf{k}}^\sigma &= \left[G_2^\sigma \left(\omega - \sigma \frac{J}{2N} \Delta \right) - G_2^\sigma(\omega) \right] \\ &\times [2t_G^\sigma(\omega) - t_E^\sigma(\omega)] \\ &- \frac{J}{2N} \left[P^\sigma \left(\omega - \sigma \frac{J}{2N} \Delta \right) - P^\sigma(\omega) \right] \\ &\times [1 + F^\sigma(\omega) t_G^\sigma(\omega)]. \end{aligned} \quad (32)$$

In addition, we have from the definition of Δ in Table I and Eqs. (15a) and (19a)

$$\begin{aligned} \Delta &= \sum_{\mathbf{k}\sigma} \sigma f(\epsilon_{\mathbf{k}\sigma}) - \frac{1}{2\pi i} \sum_{\sigma} \int_{-\infty}^{\infty} d\omega [f(\omega) - \frac{1}{2}] \\ &\times \{ [F^\sigma(\omega + i\delta)]^2 t_G^\sigma(\omega + i\delta) - [F^\sigma(\omega - i\delta)]^2 t_G^\sigma(\omega - i\delta) \}, \end{aligned} \quad (33)$$

where the sum over σ is taken in the order indicated in the definition.

Next, we must obtain explicit expression for $G_1(\omega)$, $G_2(\omega)$, $E(\omega)$, and $P(\omega)$ by using Eqs. (19) and the definitions in Table II. For example, consider $G_1(z)$, where now z denotes that we are anywhere on the complex energy plane. Using (19a), (15a), the definition of $G_1(z)$ and $F(z)$ in Table II, the partial fraction expansion

$$\begin{aligned} &\sum_{\mathbf{k}} [(\epsilon - \epsilon_{\mathbf{k}\sigma})(\omega - \epsilon_{\mathbf{k}\sigma} \pm i\delta)]^{-1} \\ &= (z - \omega)^{-1} [F(\omega \pm i\delta) - F(z)], \end{aligned} \quad (34)$$

and noting that

$$(\omega - \epsilon_{\mathbf{k}\sigma} + i\delta)^{-1} - (\omega - \epsilon_{\mathbf{k}\sigma} - i\delta)^{-1} = 2\pi i \delta(\omega - \epsilon_{\mathbf{k}\sigma}), \quad (35)$$

we obtain

$$G_1^\sigma(z) = g^\sigma(z) - \phi_G^\sigma(z), \quad (36)$$

where

$$g^\sigma(z) = \sum_{\mathbf{k}} \frac{f(\epsilon_{\mathbf{k}\sigma}) - \frac{1}{2}}{(z - \epsilon_{\mathbf{k}\sigma})} \quad (37)$$

and

$$\begin{aligned} \varphi_G^\sigma(z) &= \frac{1}{2\pi i} \int_{-\infty}^{\infty} \frac{d\omega [f(\omega) - \frac{1}{2}]}{(z - \omega)} \\ &\times \{ [F^\sigma(\omega + i\delta) - F^\sigma(z)] F^\sigma(\omega + i\delta) t_G^\sigma(\omega + i\delta) \\ &- [F^\sigma(\omega - i\delta) - F^\sigma(z)] F^\sigma(\omega - i\delta) t_G^\sigma(\omega - i\delta) \}. \end{aligned} \quad (38)$$

The subscript G on $\varphi_G^\sigma(z)$ means we use $t_G^\sigma(z)$ in Eq. (38). We note that $\varphi_G^\sigma(z)$ is a sectionally holomorphic function, i. e., discontinuous across the real axis but analytic in the upper or lower half-plane. This is because of the basic analytic properties of Cauchy integrals of this form. We can obtain $G_E^\sigma(z)$ by reversing the sign of the spin and shifting the frequency as described in Table II, viz.,

$$G_2^\sigma(z) = G_1^{\bar{\sigma}}(z + \sigma g_i \gamma + J\sigma\Delta/2N). \quad (39)$$

In a basically similar fashion, using the definitions of the sectionally holomorphic functions

$$\begin{aligned} \Phi_{G,E}^\sigma(z) &= \frac{1}{2\pi i} \int_{-\infty}^{\infty} \frac{d\omega [f(\omega) - \frac{1}{2}]}{(z - \omega)} \\ &\times \{ [F^\sigma(\omega + i\delta) - F^\sigma(z)] t_{G,E}^\sigma(\omega + i\delta) \\ &- [F^\sigma(\omega - i\delta) - F^\sigma(z)] t_{G,E}^\sigma(\omega - i\delta) \}, \end{aligned} \quad (40)$$

where the subscript G, E means that either $t_G(z)$ or $t_E(z)$ has been used, we obtain

$$(J/2N)E^\sigma(z) = (J/8N)F^\sigma(z) - \Phi_E^\sigma(z) \quad (41)$$

and

$$\begin{aligned} \frac{J}{2N}P^\sigma(z) &= \frac{J}{4N}F^\sigma \left(z + \sigma g_i \gamma + \frac{J}{2N}\sigma\Delta \right) - 2\sigma \langle S^z \rangle G_2^\sigma(z) \\ &+ \Phi_E^{\bar{\sigma}} \left(z + \sigma g_i \gamma + \frac{J}{2N}\sigma\Delta \right) - 2\Phi_G^{\bar{\sigma}} \left(z + \sigma g_i \gamma + \frac{J}{2N}\sigma\Delta \right). \end{aligned} \quad (42)$$

We point out here that all of the functions defined have the self-consistent symmetry of Eqs. (20) and (21), i. e., $[\Phi_G(z^*)]^* = \Phi_G(z)$, i. e., what we have called the reality condition holds.

At this point, in order to evaluate the basic functions $F^\sigma(z)$ and $g^\sigma(z)$, we must introduce a density of states $\rho(\epsilon_{\mathbf{k}})$ so the sums on \mathbf{k} can be done, viz.,

$$\sum_{\mathbf{k}} \rightarrow \int_{-\infty}^{\infty} d\epsilon_{\mathbf{k}} \rho(\epsilon_{\mathbf{k}}).$$

We use a Lorentzian density of states

$$\rho(\epsilon_{\mathbf{k}}) = \rho_0 D^2 / (\epsilon_{\mathbf{k}}^2 + D^2), \quad (43)$$

where ρ_0 is the density of states at the Fermi surface, $\epsilon_{\mathbf{k}} = 0$, and D is the bandwidth. By definition of the number of electrons in the conduction band we have

$$N = 2 \int_{-\infty}^{\infty} d\epsilon_{\mathbf{k}} \rho(\epsilon_{\mathbf{k}}) f(\epsilon_{\mathbf{k}}) = \pi \rho_0 D. \quad (44)$$

We note that this density of states is even in $\epsilon_{\mathbf{k}}$ (particle-hole symmetry) and in this case we obtain the symmetry relations

$$F^\sigma(z) = -F^{\bar{\sigma}}(-z) \quad (45)$$

and

$$g^\sigma(z) = g^{\bar{\sigma}}(-z). \quad (46)$$

Our Hamiltonian has this particle-hole symmetry and our truncation scheme preserves it so we also have the relations

$$t_{G,E}^\sigma(z) = -t_{G,E}^{\bar{\sigma}}(-z), \quad (47a)$$

$$\varphi_G^\sigma(z) = \varphi_G^{\bar{\sigma}}(-z), \quad (47b)$$

$$\Phi_{G,E}^\sigma(z) = -\Phi_{G,E}^{\bar{\sigma}}(-z), \quad (47c)$$

which are self-consistent. This can be seen by assuming the relations (47) and inserting them back into Eqs. (36) and (38)–(42) to obtain the other symmetries and then showing that this is consistent with the definitions of $t_{G,E}^\sigma(z)$ in Eqs. (16). These symmetry relations are tabulated in Table II. Using Eq. (43) and the definition of $F^\sigma(z)$ in Table II we obtain

$$F_+^\sigma(z) = \pi \rho_0 D / (z + \frac{1}{2}\sigma g_e \gamma + iD), \quad (48a)$$

$$F_-^\sigma(z) = \pi \rho_0 D / (z + \frac{1}{2}\sigma g_e \gamma - iD), \quad (48b)$$

where the \pm subscript notation denotes that z lies in the upper half-plane (uhp) or lower half-plane (lhp), respectively. Using this representation of the sectionally holomorphic function $F^\sigma(z)$, Eq. (45) now becomes

$$F_+^\sigma(z) = -F_-^{\bar{\sigma}}(-z) \quad (49a)$$

and

$$F_-^\sigma(z) = -F_+^{\bar{\sigma}}(-z); \quad (49b)$$

we also have

$$\begin{aligned} F_+^\sigma(z) - F_-^\sigma(z) &= (2/\pi i \rho_0) F_+^\sigma(z) F_-^\sigma(z) \\ &= -2\pi i \rho (z + \frac{1}{2}\sigma g_e \gamma). \end{aligned} \quad (50)$$

Using this notation we have

$$F^\sigma(\omega \pm i\delta) \equiv F_\pm^\sigma(\omega), \quad (51)$$

where ω is the real frequency (we shall use this \pm subscripting notation again below). The other basic function $g^\sigma(z)$ can also be evaluated now using the Lorentzian density of states, viz.,

$$g^\sigma(z) = \int_{-\infty}^{\infty} d\epsilon_{\mathbf{k}} \rho(\xi + \frac{1}{2}\sigma g_e \gamma) \frac{f(\xi) - \frac{1}{2}}{z - \xi}. \quad (52)$$

Using the partial fraction expansion

$$\begin{aligned} \frac{\rho(\xi + \frac{1}{2}\sigma g_e \gamma)}{z - \xi} &= \frac{\rho_0 D}{2i} \left[\frac{1}{z + \frac{1}{2}\sigma g_e \gamma - iD} \right. \\ &\times \left(\frac{1}{\xi - z} - \frac{1}{\xi + \frac{1}{2}\sigma g_e \gamma - iD} \right) \\ &\left. - \frac{1}{z + \frac{1}{2}\sigma g_e \gamma + iD} \left(\frac{1}{\xi - z} - \frac{1}{\xi + \frac{1}{2}\sigma g_e \gamma + iD} \right) \right], \end{aligned} \quad (53)$$

we obtain

$$\begin{aligned} g^\sigma(z) &= \frac{1}{2\pi i} F^\sigma(z) \left(\int_{-\infty}^{\infty} \frac{[f(\xi) - \frac{1}{2}] d\xi}{\xi + \frac{1}{2}\sigma g_e \gamma - iD} - \int_{-\infty}^{\infty} \frac{[f(\xi) - \frac{1}{2}] d\xi}{\xi - z} \right) \\ &- \frac{1}{2\pi i} F^\sigma(z) \left(\int_{-\infty}^{\infty} \frac{[f(\xi) - \frac{1}{2}] d\xi}{\xi + \frac{1}{2}\sigma g_e \gamma + iD} - \int_{-\infty}^{\infty} \frac{[f(\xi) - \frac{1}{2}] d\xi}{\xi - z} \right). \end{aligned} \quad (54)$$

Integrals of the form of those in Eq. (54) are done in the Appendix of the paper by Bloomfield and Hamann⁹; taking over those results, we obtain

$$\begin{aligned} g_\pm^\sigma(z) &= -\rho(z + \frac{1}{2}\sigma g_e \gamma) \psi \left(\frac{1}{2} + \frac{z}{2\pi i k T} \operatorname{sgn} \operatorname{Im} z \right) \\ &+ \frac{1}{2\pi i} \left[F^\sigma(z) \psi \left(\frac{1}{2} + \frac{D + \frac{1}{2}\sigma g_e \gamma}{2\pi k T} \right) \right. \\ &\left. - F^\sigma(z) \psi \left(\frac{1}{2} + \frac{D - \frac{1}{2}\sigma g_e \gamma}{2\pi k T} \right) \right], \end{aligned} \quad (55)$$

which is also a sectionally holomorphic function where the $+$ ($-$) subscript goes with $\operatorname{sgn} \operatorname{Im} z = +(-)$ and where $\psi(z)$ is the digamma function.²³ (Im denotes the imaginary part and sgn denotes sign of.)

The use of the Lorentzian density of states en-

ables us to express $\varphi_G^\sigma(z)$ in terms of $\Phi_G^\sigma(z)$ as follows: First, note the partial-fraction expansions

$$F_+^\sigma(\omega)/(z - \omega) = F_+^\sigma(z) \{ (z - \omega)^{-1} + [F_+^\sigma(\omega)/\pi\rho_0 D] \} \quad (56a)$$

and

$$F_-^\sigma(\omega)/(z - \omega) = F_-^\sigma(z) \{ (z - \omega)^{-1} + [F_-^\sigma(\omega)/\pi\rho_0 D] \}. \quad (56b)$$

By inserting these expressions into Eq. (40) and using Eqs. (48) and (50) we have

$$\begin{aligned} \Phi_{\pm, G}^\sigma(z) &= \frac{2}{\pi i \rho_0} F_\pm^\sigma(z) \frac{1}{2\pi i} \int_{-\infty}^{\infty} d\omega \frac{f(\omega) - \frac{1}{2}}{z - \omega} F_\mp^\sigma(\omega) t_{\mp, G}^\sigma(\omega) \\ &+ F_\pm^\sigma(z) \frac{1}{2\pi i} \int_{-\infty}^{\infty} d\omega [f(\omega) - \frac{1}{2}] \\ &\times \left(\frac{t_{+, G}^\sigma(\omega)}{\omega + \frac{1}{2}\sigma g_e \gamma + iD} - \frac{t_{-, G}^\sigma(\omega)}{\omega + \frac{1}{2}\sigma g_e \gamma - iD} \right) \end{aligned} \quad (57)$$

and, by specializing,

$$\begin{aligned} \Phi_{\pm, G}^\sigma(\pm iD - \frac{1}{2}\sigma g_e \gamma) &= \pm \frac{\pi\rho_0 D}{2\pi i} \int_{-\infty}^{\infty} \frac{d\omega [f(\omega) - \frac{1}{2}] t_{\mp, G}^\sigma(\omega)}{(\omega + \frac{1}{2}\sigma g_e \gamma \mp iD)^2} \\ &\mp \frac{\rho_0}{4} \int_{-\infty}^{\infty} d\omega [f(\omega) - \frac{1}{2}] \\ &\times \left(\frac{t_{+, G}^\sigma(\omega)}{\omega + \frac{1}{2}\sigma g_e \gamma + iD} - \frac{t_{-, G}^\sigma(\omega)}{\omega + \frac{1}{2}\sigma g_e \gamma - iD} \right), \end{aligned} \quad (58)$$

where the $+$ ($-$) subscript denotes that z lies in the uhp (lhp) and goes with $+$ ($-$) iD . Using Eq. (58) we have the expression

$$\begin{aligned} F_+^\sigma(z) \Phi_{+, G}^\sigma(iD - \frac{1}{2}\sigma g_e \gamma) + F_-^\sigma(z) \Phi_{-, G}^\sigma(-iD - \frac{1}{2}\sigma g_e \gamma) \\ = -F_+^\sigma(z) \frac{\pi\rho_0 D}{2\pi i} \int_{-\infty}^{\infty} \frac{d\omega [f(\omega) - \frac{1}{2}] t_{+, G}^\sigma(\omega)}{(\omega + \frac{1}{2}\sigma g_e \gamma + iD)^2} + F_-^\sigma(z) \frac{\pi\rho_0 D}{2\pi i} \int_{-\infty}^{\infty} \frac{d\omega [f(\omega) - \frac{1}{2}] t_{-, G}^\sigma(\omega)}{(\omega + \frac{1}{2}\sigma g_e \gamma - iD)^2} \\ + [F_+^\sigma(z) - F_-^\sigma(z)] \frac{\rho_0}{4} \int_{-\infty}^{\infty} d\omega [f(\omega) - \frac{1}{2}] \left(\frac{t_{+, G}^\sigma(\omega)}{\omega + \frac{1}{2}\sigma g_e \gamma + iD} - \frac{t_{-, G}^\sigma(\omega)}{\omega + \frac{1}{2}\sigma g_e \gamma - iD} \right). \end{aligned} \quad (59)$$

Now using the same partial-fraction expansions, Eqs. (56), we can expand $\varphi_G^\sigma(z)$ of Eq. (38) as

$$\begin{aligned} \varphi_{\pm, G}^\sigma(z) &= [F_+^\sigma(z) - F_-^\sigma(z)] \\ &\times \frac{1}{2\pi i} \int_{-\infty}^{\infty} d\omega \frac{[f(\omega) - \frac{1}{2}] F_\mp^\sigma(\omega) t_{\mp, G}^\sigma(\omega)}{z - \omega} \\ &+ F_+^\sigma(z) \frac{\pi\rho_0 D}{2\pi i} \int_{-\infty}^{\infty} \frac{d\omega [f(\omega) - \frac{1}{2}] t_{+, G}^\sigma(\omega)}{(\omega + \frac{1}{2}\sigma g_e \gamma + iD)^2} \\ &- F_-^\sigma(z) \frac{\pi\rho_0 D}{2\pi i} \int_{-\infty}^{\infty} \frac{d\omega [f(\omega) - \frac{1}{2}] t_{-, G}^\sigma(\omega)}{(\omega + \frac{1}{2}\sigma g_e \gamma - iD)^2}. \end{aligned} \quad (60)$$

So using Eqs. (60), (59), and (57) we finally obtain

$$\begin{aligned} \varphi_{\pm, G}^\sigma(z) &= F_+^\sigma(z) \Phi_{+, G}^\sigma(z) \\ &- [F_+^\sigma(z) \Phi_{-, G}^\sigma(-iD - \frac{1}{2}\sigma g_e \gamma) + F_-^\sigma(z) \Phi_{+, G}^\sigma(+iD - \frac{1}{2}\sigma g_e \gamma)]. \end{aligned} \quad (61)$$

This means that by using the Lorentzian density of states we can eliminate $\varphi_G^\sigma(z)$ and rewrite Eq. (36) as

$$\begin{aligned} G_{\pm, 1}^\sigma(z) &= g_\pm^\sigma(z) - F_+^\sigma(z) \Phi_{+, G}^\sigma(z) \\ &+ F_+^\sigma(z) \Phi_{-, G}^\sigma(-iD - \frac{1}{2}\sigma g_e \gamma) \end{aligned}$$

$$+ F^{\sigma}(z)\Phi_{+,G}^{\sigma}(iD - \frac{1}{2}\sigma g_{\theta}\gamma) . \quad (62)$$

Note that the singular terms cancel so $G_{\pm,1}^{\sigma}(z)$ is analytic in the uhp (lhp) and represents a sectionally holomorphic function.

At this point we can also evaluate Δ from Eq. (33). Note that

$$\begin{aligned} \sum_{\mathbf{k}\sigma} \sigma f(\epsilon_{\mathbf{k}\sigma}) &= 2 \int_{-\infty}^{\infty} d\omega [f(\omega) - \frac{1}{2}] \rho(\omega + \frac{1}{2}g_{\theta}\gamma) \\ &= 2 \lim_{z \rightarrow \infty} [z g_{+,}(z)] \\ &= -\frac{2N}{\pi} \operatorname{Im} \left[\psi \left(\frac{1}{2} + \frac{D - \frac{1}{2}i g_{\theta}\gamma}{2\pi k T} \right) \right] , \end{aligned} \quad (63)$$

where we have used Eqs. (55) and (44) and the properties of the digamma function. Now from Eqs. (58) and (44) and the symmetries (47) and reality conditions (tabulated in Table II) we obtain

$$\begin{aligned} \Delta &= -2N \left\{ \frac{1}{\pi} \operatorname{Im} \left[\psi \left(\frac{1}{2} + \frac{D - \frac{1}{2}i g_{\theta}\gamma}{2\pi k T} \right) \right] \right. \\ &\quad \left. - 2 \operatorname{Re} \Phi_{+,G}^{\sigma}(iD - \frac{1}{2}g_{\theta}\gamma) \right\} , \end{aligned} \quad (64)$$

where Re means the real part. There is a close connection between Δ and the total integrated conduction-electron spin density S_{σ} , viz. (see also Section III C),

$$\begin{aligned} 2S_{\sigma} &= \sum_{\mathbf{k}\sigma} \sigma \langle c_{\mathbf{k}\sigma}^{\dagger} c_{\mathbf{k}\sigma} \rangle \\ &= \sum_{\mathbf{k}\sigma} \sigma i \int_{-\infty}^{\infty} d\omega f(\omega) [\mathcal{G}_{\mathbf{k}\mathbf{k}}^{\sigma}(\omega + i\delta) - \mathcal{G}_{\mathbf{k}\mathbf{k}}^{\sigma}(\omega - i\delta)] , \end{aligned} \quad (65)$$

where we use the same σ sum convention as for Eq. (33). We now notice that because we have used a Lorentzian density of states

$$\sum_{\mathbf{k}} \frac{1}{(z - \epsilon_{\mathbf{k}\sigma})^2} = -\frac{\partial}{\partial z} F^{\sigma}(z) = \frac{[F^{\sigma}(z)]^2}{N} , \quad (66)$$

and inserting the definition of $\mathcal{G}_{\mathbf{k}\mathbf{k}}^{\sigma}(\omega \pm i\delta)$ from the solution of Eqs. (14), i. e.,

$$\mathcal{G}_{\mathbf{k}\mathbf{k}}^{\sigma}(z) = \frac{1}{2\pi} \left(\frac{1}{z - \epsilon_{\mathbf{k}\sigma}} + \frac{t_{G}^{\sigma}(z)}{(z - \epsilon_{\mathbf{k}\sigma})^2} \right) , \quad (67)$$

we obtain

$$\begin{aligned} 2S_{\sigma} &= \sum_{\mathbf{k}\sigma} \sigma f(\epsilon_{\mathbf{k}\sigma}) - \frac{1}{2\pi i N} \sum_{\sigma} \sigma \int_{-\infty}^{\infty} d\omega [f(\omega) - \frac{1}{2}] \\ &\quad \times \{ [F^{\sigma}(\omega)]^2 t_{+,G}^{\sigma}(\omega) - [F^{\sigma}(\omega)]^2 t_{-,G}^{\sigma}(\omega) \} . \end{aligned} \quad (68)$$

Defining the Pauli paramagnetic part

$$2S_{\sigma o} = \sum_{\mathbf{k}\sigma} \sigma f(\epsilon_{\mathbf{k}\sigma}) \quad (69)$$

and the rest of S_{σ} as the interaction part $S_{\sigma i}$ and using Eqs. (33) and (68), we obtain

$$\Delta = 2S_{\sigma o} + 2NS_{\sigma i} , \quad (70)$$

where

$$S_{\sigma o} = -\frac{N}{\pi} \operatorname{Im} \left[\psi \left(\frac{1}{2} + \frac{D - \frac{1}{2}i g_{\theta}\gamma}{2\pi k T} \right) \right] \quad (71)$$

and

$$S_{\sigma i} = 2 \operatorname{Re} \Phi_{+,G}^{\sigma}(iD - \frac{1}{2}g_{\theta}\gamma) . \quad (72)$$

In order to exhibit more clearly the properties of our basic Cauchy integrals $\Phi_{G,E}^{\sigma}(z)$ defined by Eq. (40), we examine the asymptotic behavior of $t_{G}^{\sigma}(z)$ and $t_{E}^{\sigma}(z)$ defined by Eqs. (16) by analytically continuing $\omega \rightarrow z$. We note that the basic properties of two-time Green's function⁴ insures that these t matrices are sectionally holomorphic and we see that

$$\lim t_{G}^{\sigma}(z) = -(J/2N) \sigma \langle S^{\sigma} \rangle + \mathcal{O}(1/z) \quad \text{as } z \rightarrow \infty , \quad (73)$$

$$\lim t_{E}^{\sigma}(z) = \mathcal{O}(1/z) \quad \text{as } z \rightarrow \infty . \quad (74)$$

If we define

$$t_{g}^{\sigma}(z) = t_{G}^{\sigma}(z) + (J/2N) \sigma \langle S^{\sigma} \rangle , \quad (75)$$

we can define a new function $\Phi_{g}^{\sigma}(z)$, which is the same as that defined by Eq. (40) but with $t_{G}^{\sigma}(z)$ replaced by $t_{g}^{\sigma}(z)$. Then by using Eqs. (50) and (52) we obtain

$$\Phi_{G}^{\sigma}(z) = \Phi_{g}^{\sigma}(z) + (J/2N) \sigma \langle S^{\sigma} \rangle g^{\sigma}(z) . \quad (76)$$

We now have a closed set of integral equations. We have the Cauchy integrals $\Phi_{G,E}^{\sigma}(z)$ of Eqs. (40) and (76), the basic functions $F^{\sigma}(z)$ and $g^{\sigma}(z)$ of Eqs. (48) and (55). The integrals must be evaluated using Eqs. (16) and (75) for the t matrices. Also the integral of Eq. (28) must be evaluated using Eqs. (32) and (70) to obtain $\langle S^{\sigma} \rangle$ and Δ (note the self-consistent conditions coming in at this stage in evaluating Δ). Finally, the t matrices are then calculated by using Eqs. (76), (62), (39), (41), and (42) in terms of the basic Cauchy integrals. Because of the nonlinear nature of Eqs. (16) and because there are products of integral operators in the numerators and denominators, we were unable to solve the resulting coupled nonlinear Hilbert boundary value problem. In zero magnetic field, $E = P$ and $G_1 = G_2$, therefore, terms cancel in the numerator and denominator and $3t_E = 2t_G$. This case has been solved by the Hilbert method.^{9,24} To solve our integral equations in nonzero field we have essentially converted the problem into a set of simultaneous nonlinear equations for the t 's evaluated at a finite number of points along the imaginary axis. This technique has been previously discussed by two of us.²⁰ The details of its application herein are contained in the Appendix. We have carried out the calculations using parameters appropriate to systems like CuFe , i. e., an antiferromagnetic coupling constant $J < 0$ corresponding to a Kondo temperature $T_K = 16^{\circ}$, $\epsilon_F = 4.7$ eV, and the bandwidth $D = 1$ eV. As indicated above we

have considered only the spin- $\frac{1}{2}$ case and we assumed equal g factors for impurity spin and conduction-electron spin, $g_i = g_e = 2$. From the solutions of this set of equations we are able to calculate all of the quantities of physical interest. Our method and results are presented in Sec. III.²⁵

III. RESULTS

A. Resistivity

The longitudinal conductivity is given by²⁶

$$\sigma_L = -\frac{1}{3}e^2 \int_{-\infty}^{\infty} d\epsilon \rho(\epsilon) v^2(\epsilon) \sum_{\sigma} \tau_{\sigma}(\epsilon) \frac{\partial f^{\sigma}}{\partial \epsilon}, \quad (77)$$

where $\rho(\epsilon)$ is the density of states given by Eq. (43), $v(\epsilon)$ is the electronic velocity, $\tau_{\sigma}(\epsilon)$ is the relaxation time for an electron of spin σ , and $f^{\sigma} \equiv f(\epsilon + \frac{1}{2}\sigma g_e \gamma)$ is the Fermi distribution function. Note that each spin distribution obeys its own transport equation and, therefore, has its own relaxation time and equilibrium distribution. At low temperatures $\partial f^{\sigma}/\partial \epsilon$ has its peak at $\epsilon = -\frac{1}{2}g_e \gamma$ because of our convention that spin-up electrons have lower energy. The relaxation time for low impurity concentration is given by

$$\begin{aligned} \tau_{\sigma}(\epsilon) &= \hbar \rho_0 \{2CN \operatorname{Im} [-\rho_0 t_C^{\sigma}(\epsilon + i\delta)]\}^{-1} \\ &= 1.057 \times 10^{-16} \{CD \operatorname{Im} [-\rho_0 t_C^{\sigma}(\epsilon + i\delta)]\}^{-1}, \end{aligned} \quad (78)$$

where we have made use of Eq. (44) for N . Here, C is the fractional concentration and D is the bandwidth which we take as 1 eV in these calculations. The density of states at the Fermi surface is taken from free-electron considerations and is given by

$$\rho_0 = \frac{(2m)^{3/2} \epsilon_F^{1/2}}{2\pi^2 \hbar^3} = 2.92 \times 10^4 \text{ (eV)}^{-1} \quad (79)$$

and

$$\epsilon_F = 3\pi D/2 = 4.712 \text{ eV} \quad (80)$$

with m as the free-electron mass. These values of the parameters are used throughout this calculation. The square of the electronic velocity is given by

$$v^2(\epsilon) \approx 2(\epsilon_F + \epsilon)/m = (3\pi D + 2\epsilon)/m. \quad (81)$$

At the temperatures of interest, the sharpness of the Fermi function relative to the slow variation of the rest of the integral in Eq. (77) means that to a good approximation we can write the resistivity as

$$\rho_L = \sigma_L^{-1} \approx (m/Ne^2) [\tau(-\frac{1}{2}g_e \gamma) + \tau(\frac{1}{2}g_e \gamma)]^{-1}. \quad (82)$$

If an impurity potential scattering term had been included in our original Hamiltonian, for example, a point potential scattering term of the form

$$V \sum_{\mathbf{k}\mathbf{k}'} c_{\mathbf{k}\sigma}^{\dagger} c_{\mathbf{k}'\sigma}, \quad (83)$$

it would have the effect of breaking the particle-hole symmetry. There would also be a transverse re-

sistivity and Hall coefficient given by

$$\rho_T = \sigma_T (\sigma_T^2 + \sigma_{TH}^2)^{-1}, \quad (84)$$

and

$$R = H^{-1} \sigma_{TH} (\sigma_T^2 + \sigma_{TH}^2)^{-1}, \quad (85)$$

where

$$\sigma_T = \sigma_i (1 + \omega_0^2 \tau_i^2)^{-1} + \sigma_e (1 + \omega_0^2 \tau_e^2)^{-1}, \quad (86a)$$

$$\sigma_{TH} = \omega_0 \sigma_i \tau_i (1 + \omega_0^2 \tau_i^2)^{-1} + \omega_0 \sigma_e \tau_e (1 + \omega_0^2 \tau_e^2)^{-1}. \quad (86b)$$

$\omega_0 = eH/mc$ is the cyclotron frequency, σ_i is given by the appropriate part of Eq. (77), and τ_i is given by Eq. (78) with $\epsilon = \mp \frac{1}{2}g_e \gamma$, respectively. In order to shorten the calculation done here and yet retain the physical effects of the field on exchange scattering, we set $V = 0$, no potential scattering, so that $\rho_T = \rho_L = \rho$ and R is a constant. Then, making use of the particle-hole symmetry given in Table II we have

$$\rho \approx m [2Ne^2 \tau_i (-\frac{1}{2}g_e \gamma)]^{-1}. \quad (87)$$

In the calculation of More¹⁷ potential scattering was included and a T - and H -dependent Hall coefficient was obtained.

Figure 1 shows the results for the resistivity in the form

$$\rho N / DC = 0.1866 \times 10^9 \operatorname{Im} [-\rho_0 t_C^{\sigma} (-\frac{1}{2}g_e \gamma + i\delta)] \quad (88)$$

as a function of temperature T for a number of

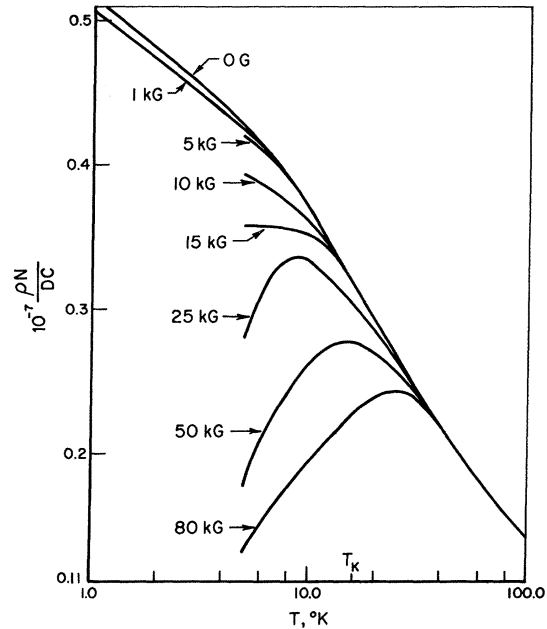


FIG. 1. Resistivity ρ as a function of temperature for a number of external magnetic fields, N is the number of unit cells in the lattice and C is the impurity concentration.

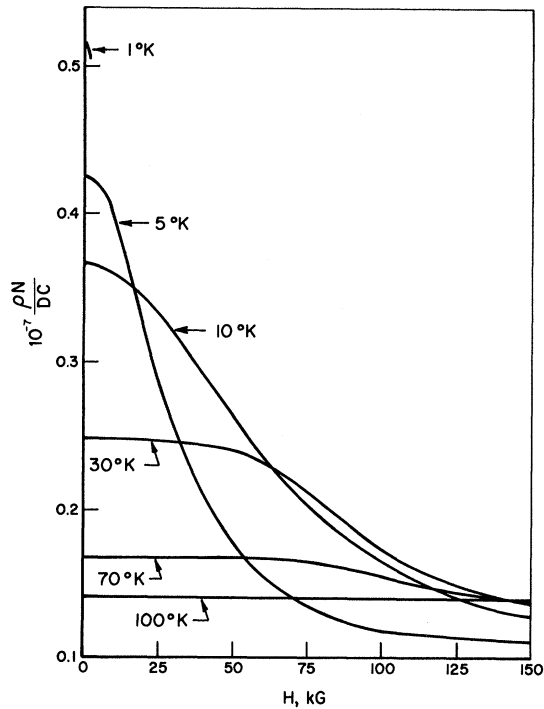


FIG. 2. Resistivity ρ as a function of external magnetic field for a number of temperatures.

values of the external magnetic field. Figure 2 shows the same results as a function of the external field H . Note that the Kondo temperature $T_K = 16^\circ\text{K}$. Both Figs. 1 and 2 show that the applied magnetic field tends to suppress the anomalous resistivity which results from exchange scattering below T_K . The "freezing out" of the spin-flip scattering process can be understood by considering two competing mechanisms. The initial rise of the resistivity as the temperature decreases through T_K results from an enhancement of the spin-flip scattering process due to a decrease in the thermal fluctuations of both spin systems. For $H=0$, only this mechanism obtains. However, in the presence of an external H field, a further decrease in temperature enables the Zeeman splittings to significantly influence the population distribution in each spin system. At sufficiently high values of H/T , this population difference between the spin-up and the spin-down state will become sufficiently large and inhibit the spin-flip scattering process. The scattering of conduction electrons from spin up to spin down is inhibited by a depopulation of the spin-down impurity-spin energy level by the field, and the scattering of spin down to spin up is inhibited by a depopulation of spin-down conduction-electron levels. Comparing Fig. 1 to the experimental results of Monod¹⁶ for CuFe , for which $T_K \approx 16^\circ\text{K}$, we note that the cal-

culated field dependence of the resistivity is too strong, i. e., the negative magnetoresistance is too large, especially at lower temperatures. This is apparently the result of the truncation process. A perturbation treatment of this problem leads to logarithmic divergence of all orders and the Nagaoka truncation in effect only sums up the leading logarithmic terms.²⁷ The higher-order terms that must come in at lower temperatures are neglected. As the truncation scheme used in this calculation is a simple generalization of Nagaoka, it is expected to suffer from the same defects. However, the expression for $\langle S^z \rangle$ in Eq. (27) is exact. Thus, we expect the field effects to be somewhat overemphasized to the extent that our truncation approximation does not allow the correlation function $\langle s^+ s^- \rangle$, which is used in the expression for $\langle S^z \rangle$, to become as negative and as large as it should. On the other hand, for low fields and very low temperatures $\langle s^+ s^- \rangle$ becomes too large as is discussed in Sec. IIIB. The many-body effects may be seen in Fig. 3 which shows $\text{Im}[\rho_0 t^+(\omega)]$ as a function of $\omega D/kT$ for $T = 5^\circ\text{K}$ and a number of fields. The $H=0$ curve is obtained for the Nagaoka truncation scheme; third-order perturbation theory would give a negative divergence instead of a negative trough. As the field is increased the trough moves to the left and the many-body effects can be seen to influence the line shape near the Fermi level, $\omega = 0$. The effect is to retard the higher-field curves from departing rapidly from the $H=0$ curve. This tends to make

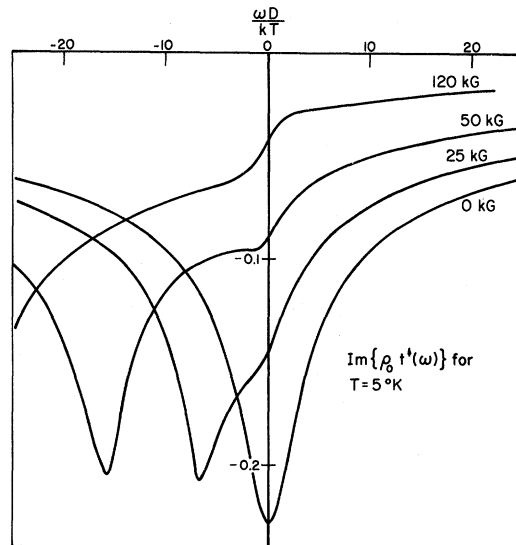


FIG. 3. Imaginary part of the t matrix t_G for spin-up electrons at 5°K as a function of the real frequency ω for a number of external magnetic fields; $\omega=0$ corresponds to the Fermi energy.

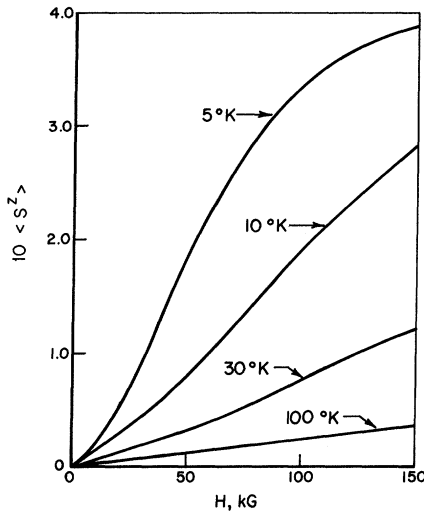


FIG. 4. Thermal average of the impurity spin $\langle S^z \rangle$ as a function of the external magnetic field for a number of temperatures.

the negative magnetoresistance smaller and presumably it is this effect that is underestimated by the truncation scheme. However, the calculated magnetoresistance qualitatively follows experiment and it is expected to be quantitatively more valid for low fields except for very low temperatures as discussed below. The recent singlet-ground-state calculation of Ishii²⁸ yields a magnetoresistivity similar to our results in Fig. 2. The complex behavior in More and Suhl's curves¹⁷ referred to by Ishii is a result of their numerical approximations.²⁹

B. Magnetization

The excess magnetization over that of the pure sample is given by

$$M = \mu_B (g_i \langle S^z \rangle + g_e S_{ei}), \quad (89)$$

where $\langle S^z \rangle$ is given by Eq. (27) and S_{ei} by Eq. (72). The results for $\langle S^z \rangle$ are shown in Fig. 4. Since Eq. (27) is exact, the effect of the exchange scattering is only felt through the correlation function $\langle s^+ s^- \rangle$. The results of our calculation for $\langle s^+ s^- \rangle$ are shown in Figs. 5 and 6. We note that $\langle s^+ s^- \rangle$ is negative and becomes, in general, more negative the lowers the temperature and field. There is a reversal of this trend at higher fields when the temperature is lowered as is evident in Fig. 6. This may be attributed to the absence of thermal fluctuations at low temperatures. The strong direct coupling of the localized spin to the field is then dominant and the spin-spin scattering is suppressed. At low fields, our theory breaks down as the temperature goes below 0.5°K. For ex-

ample, at 1°K and 100 G, our calculation easily converged to $\langle S^z \rangle = 3.2 \times 10^{-4}$. At 0.1°K and 100 G, an initial zero- $\langle S^z \rangle$ yielded $\langle s^+ s^- \rangle = -0.699$ and upon iteration we find a relatively large negative $\langle S^z \rangle$ (-0.013). Oscillations in $\langle S^z \rangle$ above and below zero occur and no convergence obtains. (See the Appendix for a discussion of our iterative procedure.) This nonphysical result follows from Eq. (27) if $\langle s^+ s^- \rangle < -0.5$, and can already be forecast from Zittartz's³⁰ zero-field low- T calculation which yields $\langle s^+ s^- \rangle \approx -\frac{2}{3}$. Dividing by $J\Delta/N$ and taking the zero-field limit of Eq. (32) gives Zittartz's formula.³⁰ Also note the high-field high-temperature saturation levels $\langle s^+ s^- \rangle \sim -0.138$, which indicate that high fields and temperatures do not completely eliminate the exchange scattering effects which tend to reduce $\langle S^z \rangle$.

The results for S_{ei} are shown in Fig. 7 as a function of field for various temperatures. Note that it is negative; this tends to reduce the conduction-electron spin alignment with $\langle S^z \rangle$ (which points up). Its magnitude increases as the temperature is lowered and the field is raised. Also for the same temperature and field ranges, it is about an order of magnitude less in absolute value than $\langle S^z \rangle$. This can be better appreciated by a calculation to first order in the coupling constant, the relevant parameter being $J_0/N = -0.14429$. Consider Eq. (72) and take the dominant part of $t_0^g(\omega)$ from Eq. (16a),

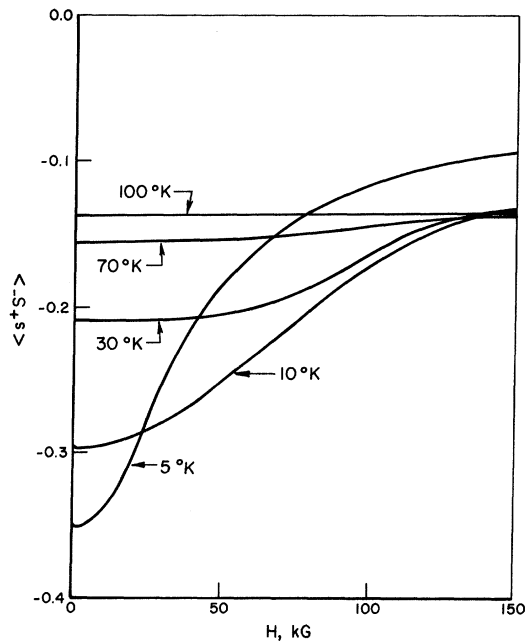


FIG. 5. Correlation functions $\langle s^+ s^- \rangle$ as a function of the external magnetic field for a number of temperatures.

$$t_G^a(\omega) \approx -(J/2N)\sigma \langle S^z \rangle, \quad (90)$$

which is the same as the high-energy limit given in Eq. (73), and insert this into Eq. (40) for $\Phi_{+,G}$ ($iD - \frac{1}{2}g_e\gamma$) to obtain

$$\begin{aligned} S_{ei} &\approx 2 \operatorname{Re} \left(\frac{J}{2N} \langle S^z \rangle \int_{-\infty}^{\infty} \frac{d\omega [f(\omega) - \frac{1}{2}]}{iD - \frac{1}{2}g_e\gamma - \omega} \rho(\omega + \frac{1}{2}g_e\gamma) \right) \\ &= \frac{J}{N} \langle S^z \rangle \operatorname{Re} g_i^! (iD - \frac{1}{2}g_e\gamma) \\ &= \frac{J\rho_0 D}{2N} \langle S^z \rangle \operatorname{Re} \left(\frac{\partial \psi(\frac{1}{2} + z/2\pi kT)}{\partial z} \Big|_{z=D+1/2ig_e\gamma} \right) \\ &\approx (J\rho_0/2N) \langle S^z \rangle, \end{aligned} \quad (91)$$

where we have used Eqs. (48) and (52) and, in the last step, the asymptotic expansion of the digamma function.²³ This result and the results shown in Fig. 7 indicate that the conduction-electron contribution to the bulk impurity susceptibility is smaller by about an order of magnitude than the impurity spin contribution. Also the form of $\langle S^z \rangle$ and the size of S_{ei} indicates that the reduction of effective moment is mainly due to a failure of the local spin to align in the field because of the strong spin correlations between impurity and conduction electrons and not due to a spin-compensating conduction-electron polarization cloud surrounding the impurity. This is in agreement with the calculation of Klein.¹⁸

We may compare these results to previous calculations and to experimental data. In the *CuFe* alloy system, Heeger *et al.*¹⁰ have compared the temperature dependence of the excess susceptibility obtained from bulk susceptibility measurements with that inferred from the Fe^{57} Mössbauer data. At temperatures well above T_K the impurity hyperfine field H_{int} scales with the excess sus-

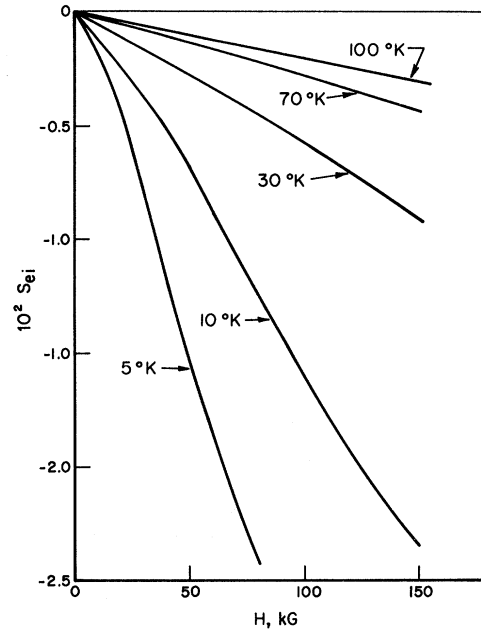


FIG. 7. Interaction part of the total integrated conduction-electron spin density S_{ei} as a function of external magnetic field for a number of temperatures.

ceptibility χ_{imp} , but below T_K it deviates markedly. These authors argued that at high temperatures only the bare impurity susceptibility is present and the above-mentioned data in this temperature region gives a reliable measure of the slope of H_{int} versus χ_{imp} . This slope is then used below T_K to predict $\chi_{imp \text{ Moss}}$ from the Mössbauer data. They find that at very low temperature $\chi_{imp \text{ Moss}}$ is

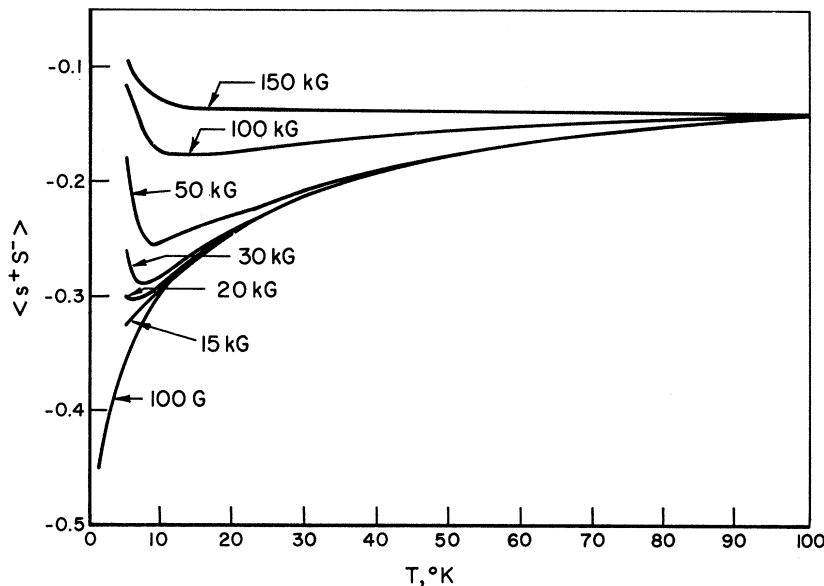


FIG. 6. Correlation function $\langle S^z S^z \rangle$ as a function of the temperature for a number of external magnetic fields.

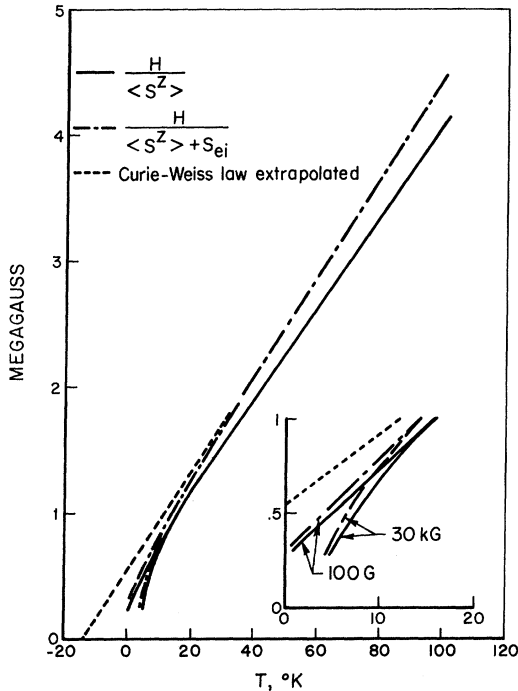


FIG. 8. Two quantities proportional to the external field H divided by the excess magnetization, $H/(\langle S^z \rangle + S_{ei})$, and H divided by the impurity magnetization, $H/\langle S^z \rangle$, as a function of temperature for a low field $H=100$ G and a high field $H=30$ kG; a Curie-Weiss law extrapolated from the high temperature yields a Néel temperature of ~ 13.5 °K to compare to a Kondo temperature of 16 °K; the low-temperature detail is shown in the insert.

approximately half the excess susceptibility χ_{imp} obtained directly by susceptibility measurements and thus infer that the conduction-electron contribution to the total excess susceptibility is equal to the local impurity susceptibility. They also did a calculation based on the variational model of Appelbaum and Kondo⁷ from which they obtain an S_{ei} of the same magnitude and sign as $\langle S^z \rangle$ in disagreement with the results of the calculation done here. On the other hand, low-temperature deviations between the impurity hyperfine field and the excess susceptibility have also been found by Narath, Brog, and Jones³¹ in $MoCo$ alloys. However, in this case the deviations are a monotonic function of the impurity concentration and may be expected to result in some way from impurity-impurity interactions. Also Stassis and Shull³² measure the impurity magnetic moment by polarized neutron scattering in $CuFe$ and conclude that the magnetic scattering amplitude data has, within experimental error, the same temperature dependence as the bulk susceptibility measured on the same samples. This would indicate only a small

conduction-electron contribution in agreement with the calculation done here. The predicted positive resonance shifts by Heeger *et al.*¹⁰ are contradicted by the Narath and Gossard³³ NMR observations on $Au(Ag)V$ alloys. They conclude that there is a very small *reduction* in the impurity spin susceptibility. These results are also consistent with our theory. Also, as evidenced by the calculated high-field and high-temperature saturation value attained by $\langle s^+s^- \rangle$ (see Fig. 6), an assumption of complete suppression of exchange scattering effects at high temperatures, i. e., $T \gg T_K$, is questionable. Ishii²⁸ in his recent zero-temperature variational calculation in which he treats the magnetic field as only interacting directly with the localized spin finds the result in Eq. (91) for the total localized spin [see Eq. (101)]; he also points out that the calculations in Ref. 10 are in disagreement with this.

Figure 8 presents our results for equal g factors for $2H/\mu_B M$ (which is related to the bulk χ_{imp}) and $H/\langle S^z \rangle$ (which is related to χ_{imp} Moss) as a function of temperature for $H=100$ G and $H=30$ kG. We see that for high temperatures, M follows a Curie-Weiss law of the form $H(T+T_c)^{-1}$ with $T_c \approx 13.5$ °K to compare with a Kondo temperature $T_K=16$ °K. Below T_K we note deviation even for $H=100$ °C. These deviations might be described by $H/\langle S^z \rangle \sim T^x$ with $x < 1$. There is experimental evidence for this trend,³⁴ at least for fields $H < 1$ kG, namely, that below 1 °K, $x = \frac{1}{2}$. In our calculation, this trend increases with the field strength. It has been suggested that such behavior is due to the formation of impurity clumps,¹¹ but our results indicate that it may be inherent in the single impurity problem. We also find that below T_K , $\langle S^z \rangle$ increases faster than linear, approaching saturation more rapidly. It is interesting to note that when Osaka³⁵ calculated χ at zero-field from Suhl's theory,² his result was identical to Hamann's⁸ as is to be expected from the equivalence³⁶ between the Nagaoka and Suhl theories. These calculations differ from ours and those of Shastry and Ganguly³⁷ who used the solution⁹ to calculate the zero-field susceptibility. They found $x=0.6$ and curves similar to our low-field curves.

C. Electron Spin and Number Density

The conduction-electron density for spin σ as a function of r , the radial distance from the impurity site, is given by

$$\rho_\sigma(r) = N^{-1} \sum_{\mathbf{k}\mathbf{k}'} \exp[i(\mathbf{k} - \mathbf{k}') \cdot \mathbf{r}] \langle c_{\mathbf{k}\sigma}^\dagger c_{\mathbf{k}'\sigma} \rangle. \quad (92)$$

Using the definition in Table I and Eq. (17), we have

$$\langle c_{\mathbf{k}\sigma}^\dagger c_{\mathbf{k}'\sigma} \rangle = i \int_{-\infty}^{\infty} d\omega f(\omega) [G_{\mathbf{k}\mathbf{k}'}^\sigma(\omega + i\delta) - G_{\mathbf{k}\mathbf{k}'}^\sigma(\omega - i\delta)], \quad (93)$$

where from Eqs. (14a), (15), and (16a) we obtain

$$g_{\vec{k}\vec{k}'}^{\sigma} = [2\pi(\omega - \epsilon_{\vec{k}\sigma})]^{-1} [\delta_{\vec{k}\vec{k}'} + (\omega - \epsilon_{\vec{k}\sigma})^{-1} t_G^{\sigma}(\omega)], \quad (94)$$

thus we can define

$$m_{\sigma}(\omega + i\delta, \vec{r}) = \sum_{\vec{k}} \frac{\exp(i\vec{k} \cdot \vec{r})}{\omega + i\delta - \epsilon_{\vec{k}\sigma}} \quad (95)$$

and using this definition and Eq. (18) we can express the electron density as

$$N\rho_{\sigma}(r) = \sum_{\vec{k}} f(\epsilon_{\vec{k}\sigma}) - \pi^{-1} \int_{-\infty}^{\infty} d\omega [f(\omega) - \frac{1}{2}] \\ \times \text{Im}[m_{\sigma}^2(\omega + i\delta, k)t_G^{\sigma}(\omega + i\delta)]. \quad (96)$$

We can perform the angle integration in Eq. (95) to obtain for the free-electron case

$$m_{\sigma}(\omega + i\delta, r) = \frac{1}{2\pi^2} \int_0^{\infty} k^2 dk \frac{\sin kr}{kr} \frac{1}{(\omega + i\delta - \epsilon_{\vec{k}} + \frac{1}{2}\sigma\gamma g)}. \quad (97)$$

We then change variables assuming that the main contribution to the integral comes from the energy region around the Fermi energy $\epsilon_{\vec{k}} = 0$. We use

$$k = [2m(\epsilon_F + \epsilon_k)]^{1/2} \approx k_F [1 + (\epsilon_k/2\epsilon_F)], \quad (98)$$

where $k_F = (2m\epsilon_F)^{1/2}$ and ϵ_k , $D \ll \epsilon_F$. After substituting our Lorentzian density of states $\rho(\epsilon_k) d\epsilon_k$ for $k^2 dk$ we have

$$m_{\sigma}(\omega + i\delta, r) \\ = \frac{\rho_0 D^2}{2\pi^2} \frac{1}{k_F r} \\ \times \int_{-\infty}^{\infty} d\epsilon \frac{\sin[k_F r(1 + \epsilon/2\epsilon_F)]}{(\epsilon^2 + D^2)(1 + \epsilon/2\epsilon_F)(\omega + i\delta - \epsilon + \frac{1}{2}\sigma\gamma g)}. \quad (99)$$

We evaluate this integral by contour integration expressing the sine function in terms of exponentials and closing the contour in the upper- or lower-half complex ϵ planes where appropriate. Using the fact that in the free-electron case $D/2\epsilon_F = 1/3\pi$, we have

$$m_{\sigma}(\omega + i\delta, r) = -\frac{F_{\frac{1}{2}}^{\sigma}(\omega)}{2ik_F r} \exp\left(-ik_F r - \frac{k_F r}{3\pi}\right) \\ + \frac{F_{\frac{1}{2}}^{\sigma}(\omega)}{2ik_F r} \exp(ik_F r) \left[\exp\left(-\frac{k_F r}{3\pi}\right) \right. \\ \left. - 2iDF_{\frac{1}{2}}^{\sigma}(\omega) \exp\left(\frac{ik_F r(\omega + \frac{1}{2}\sigma\gamma g)}{3\pi D}\right) \right], \quad (100)$$

where $F_{\frac{1}{2}}^{\sigma}(\omega)$ is given by Eq. (48). This expression is then used in Eq. (96) where the integral is evaluated in a manner similar to that described in the Appendix.

From Table I and Eqs. (68), (92), and (93) we find relations between the spin density at the origin, the integrated electron spin density, and Δ :

$$\rho_s(0) = (1/N) \sum_{\vec{k}} n_{\vec{k}\sigma}, \quad \Delta = N[\rho_s(0) - \rho_s(0)], \\ 2S_{eo} = N[\rho_{s0}(0) - \rho_{s0}(0)], \quad 2S_{et} = \rho_{s,et}(0) - \rho_{s,et}(0) \equiv \delta\rho(0). \quad (101)$$

Asymptotic expansion of the digamma function²³ for low temperatures and nonenormous fields yields from Eq. (71)

$$S_{eo} \approx N\{\pi^{-1} \arctan(g\gamma/2D) + 2g\gamma k T [4D^2 + (g\gamma)^2]^{-1}\} \\ \approx 0.5 \rho_0 g\gamma.$$

Then the field-dependent energy shift [see Eqs. (14c) and (39)] from Eqs. (70) and (91),

$$g\gamma + \frac{J}{2N} \Delta \approx g\gamma \left(1 + 0.5 \frac{J\rho_0}{N}\right) + \left(\frac{J\rho_0}{N}\right)^2 \pi D \langle S^z \rangle.$$

The last term resulting from S_{et} (or the interaction part of the spin density) dominates this expression. Thus, the energy shift depends most strongly on $\delta\rho(0)$ which is proportional to the density of electron states at the Fermi surface times the dominant part of the t matrix in finite field [see Eqs. (90) and (91)].

Our results for the spin density $\delta\rho(r)$ and charge density (neglecting the uniform background) are given in Figs. 9 and 10. Figure 9(a) shows an example of the spin density times $(k_F r)^2$ as a function of $k_F r$ for $T = 10^\circ \text{K}$, $H = 150 \text{ kG}$ and Fig. 9(b) shows the corresponding charge density. Figure 10 is a graph of the envelope of the positive and negative maxima of the spin-density curves times $(k_F r)^2$ normalized by $\langle S^z \rangle$ for various temperatures and fields. The curves A and D are for $T = 1^\circ \text{K}$, $H = 100 \text{ G}$ or 1 kG as the curve for the two different fields are indistinguishable. Likewise, the curves B and E are for $T = 10^\circ \text{K}$, $H = 100 \text{ G}$ and C and F are for $T = 10^\circ \text{K}$, $H = 150 \text{ kG}$ or $T = 100^\circ \text{K}$, $H = 100 \text{ G}$ or 150 kG . Qualitatively, the temperature and field dependences of the spin density are the same as those of $\langle S^z \rangle$ —increasing in strength as H increases and T decreases. The extent to which these curves do not coincide indicates extra temperature and field dependence apart from that of $\langle S^z \rangle$. A number of the features of these results can be seen to arise from certain terms of Eqs. (100) and (96). The square of m_{σ} is the immediate source of the long-range oscillatory terms such as $(k_F r)^{-2} \cos(2k_F r)$, as well as exponentially damped terms such as $(k_F r)^{-2} \exp(-k_F r/3\pi) \sin^2(k_F r)$. The ω integration of Eq. (96) modifies these simple dependencies in two ways. First, we obtain a temperature-dependent damping, $\exp(-\lambda)$, where λ is proportional to $k_F r \pi k T / \epsilon_F$, as can be seen by considering the poles of $[f(\omega) - \frac{1}{2}]$ on the imaginary axis close to $\omega = 0$.

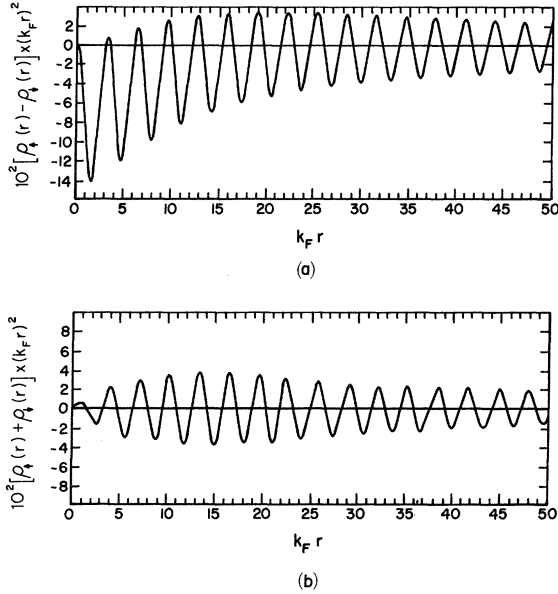


FIG. 9. (a) Spin density times $(k_F r)^2$ as a function of $k_F r$ for temperature, $T=10^\circ\text{K}$ and external magnetic field, $H=150\text{ kG}$; (b) charge density times $(k_F r)^2$ as a function of $k_F r$ for the same temperature and field. [For 100 G, curve (b) is essentially the same, while curve (a) is scaled down by $\langle S^z \rangle$ ratio $\approx 5 \times 10^{-5}$.]

For the values of $0 < k_F r \leq 80$ and T considered here, this damping is negligible. Second, the $(k_F r)^{-2}$ dependence is altered. A perturbation treatment of our formalism for small J/N and for $kT \ll \epsilon_F$ yields the RKKY¹³ result $\langle S^z \rangle (k_F r)^{-3} \cos(2k_F r)$ for the spin density and the result $\langle S^z \rangle (k_F r)^{-3} \sin(2k_F r)$ for the charge density. However, our numerical calculation yields results intermediate between $(k_F r)^{-2}$ and $(k_F r)^{-3}$. We have the dependence $(k_F r)^{-n-2}$, where $n=0.55$ for curves A and D in Fig. 10, $n=0.67$ for curves B and E and $n=0.80$ for curves C and F, n decreasing as T and H are lowered. It is interesting to note that, if this effect is real, it implies that the interaction between two magnetic impurities, via the electron spin-density overlap, increases as T decreases.

We obtain a negative definite component in the spin polarization as seen in Figs. 9(a) and 10. This is damped out by the term in Eq. (100), $\exp(-k_F r/3\pi)$. The negative definite component essentially disappears at $k_F r=25$, which for Cu corresponds to about 10 lattice spacings. Other densities of states or band structure would change slightly the numerical factor $D/2\epsilon_F$ (equal to $1/3\pi$ here), which determines this range. Contrary to the long-range sinusoidal behavior which reflects the sharpness of the Fermi surface, the short-range character of the negative definite part of the electron spin-density results from the bandwidth D , satisfying

$$kT \ll D \ll \epsilon_F.$$

The charge-density oscillations have, however, only sinusoidal behavior and even though $\rho_s(r)$ and $\rho_c(r)$ separately are H and T dependent, the charge density has little H and T dependence. This charge density is the result of the local inhomogeneous effective magnetic field provided by the impurity spin which changes the density of states locally. As seen from Eqs. (68) and (101) and the symmetries in Table II, the charge density $[\rho_{s,ei}(0) + \rho_{c,ei}(0) = 0]$ exactly vanishes at the impurity site for all values of H and T . This is the same result found by Ishii.²⁸

The results obtained here disagree with the calculation of Heeger *et al.*¹⁰ which predicts a long-range nonoscillatory component in the spin polarization. Their spin polarization had a long-range component that was of the same form as the various correlation function calculations,^{3,6} i. e., $[\sin(2k_F r)/r]^2$. Any nonoscillatory long-range component such as this should show up in a shift in the host NMR results. Experimental results on $\text{Au}(\text{Ag}) V$ by Narath and Gossard³³ indicate no such shift exists. Later experimental work by Golibersuch and Golibersuch and Heeger³⁸ on CuFe also shows no shift. The fact that any nonoscillatory component in the spin polarization is undetectable in the host NMR indicates that it is short range and this is in agreement with our calculations. This agreement indicates that this particular experiment will not differentiate between the validity of the $s-d$ and virtual state models as previously

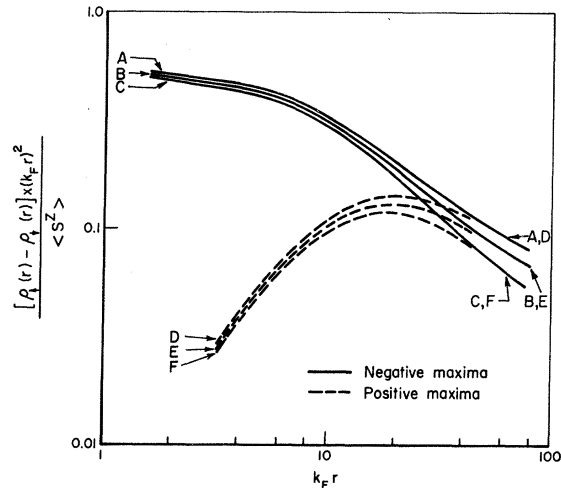


FIG. 10. Relative maxima of the spin density times $(k_F r)^2$ normalized by $\langle S^z \rangle$ as a function of $k_F r$ for various temperatures and fields: (A and D) $T=1^\circ\text{K}$ for $H=100\text{ G}$ or 1 kG (curves for the two different fields are indistinguishable); (B and E) $T=10^\circ\text{K}$ for $H=100\text{ G}$; (C and F) $T=10^\circ\text{K}$ for $H=150\text{ kG}$ or $T=100^\circ\text{K}$ for $H=100\text{ G}$ or $H=150\text{ kG}$.

thought.³⁹ Calculation with the virtual state model⁴⁰ gives no nonoscillatory spin-polarization contribution and our calculation with the s - d model gives the nonoscillatory component too short range to detect. Also both models give charge-density oscillations.

IV. CONCLUSIONS

We summarize the main results and conclusions of this paper as follows:

(a) A comparison of our magnetoresistance results with experiment^{16,41} is favorable but indicates that the low-temperature high-field effects are over-emphasized in our calculations. This is probably due to the truncation approximation applied to the equations of motion.

(b) Our results for $\langle s^+s^- \rangle$ indicate that significant effects of exchange scattering persist even at high temperatures and fields. For low fields as $T \rightarrow 0$ we find unphysical values for $\langle s^+s^- \rangle$. This is a defect in the decoupling procedure which already showed up in the zero-field calculation of the specific heat²⁴ and susceptibility.³⁰

(c) The fact that we find S_{ei} to be an order of magnitude less than and opposite in sign to $\langle S^z \rangle$ indicates that there is no large contribution of the conduction electrons to the impurity susceptibility. This is in agreement with the latest experimental results³¹⁻³³. We also conclude that the apparent disappearance of the effective moment as temperature is decreased is due to the strong spin correlations between the impurity and conduction electrons and not due to a spin-compensating conduction-electron polarization cloud. This is in agreement with the calculation of Klein.¹⁷

(d) Our plots of magnetization in the form H/M given in Fig. 8 show an extrapolated Curie-Weiss behavior with a Néel temperature $T_c \approx 13.5$ °K to compare with a Kondo temperature $T_K = 16$ °K.

There is a low-temperature, $T < T_K$, deviation from the Curie-Weiss behavior in the direction of increasing susceptibility which increases with field. This behavior appears to be inherent in the single impurity model and cannot be due to impurity clumping.

(e) Our results for the spin polarization show that there is no long-range nonoscillatory component that could be detectable by host NMR experiments. The nonoscillatory component is exponentially damped by a factor that depends on the ratio of the conduction-electron bandwidth to the Fermi energy. The charge density is purely oscillatory, is essentially independent of T and H , and vanishes at the impurity site.

ACKNOWLEDGMENTS

The authors would like to thank Professor A. Heeger, Dr. C. Stassis, Dr. K. Brog, and Dr. M. L. Glasser for many helpful discussions. Also, we would especially like to thank Dr. K. Petzinger for critical comments on our truncation scheme and our method of calculating $\langle S^z \rangle$.

APPENDIX

The Cauchy integrals that have to be evaluated are all of the form

$$I = \int_{-\infty}^{\infty} d\omega [f(\omega) - \frac{1}{2}] [\gamma(\omega + i\delta) - \gamma(\omega - i\delta)], \quad (\text{A1})$$

where $\gamma(z)$ is a sectionally holomorphic function represented by $\gamma_{\pm}(z)$ as in the theory section. In order to do this we use the procedure of Bloomfield and Sievert²⁰ and express the Fermi function in terms of digamma functions and then expand these digamma functions by using their recursion relations and asymptotic expansions. We obtain

$$I \approx -\frac{kT}{D} \int_{-\infty}^{\infty} dx \gamma(x + i\delta) \left[\sum_{n=1}^N \frac{1}{x - i\pi(kT/D)(2n-1)} + \frac{1}{2(x - iP)} - \frac{i\pi kT}{6D} \left(\frac{1}{x - iP} \right)^2 + \frac{1}{2\pi i(kT/D)} \ln \left(\frac{2N+1}{2} + \frac{ix}{2\pi(kT/D)} \right) \right] \\ + \frac{kT}{D} \int_{-\infty}^{\infty} dx \gamma(x - i\delta) \left[\sum_{n=1}^N \frac{1}{x + i\pi(kT/D)(2n-1)} + \frac{1}{2(x + iP)} + \frac{i\pi kT}{6D} \left(\frac{1}{x + iP} \right)^2 - \frac{1}{2\pi i(kT/D)} \ln \left(\frac{2N+1}{2} - \frac{ix}{2\pi(kT/D)} \right) \right], \quad (\text{A2})$$

where $x = \omega/D$ and $P = \pi(kT/D)(2N+1)$. Note that the terms of the asymptotic expansions retained have a single and double pole at $\pm iP$ and we have dropped the next term $[120(x \pm iP)^4]^{-1}$ and those having higher-order poles. The error made by representing the Fermi function on the real axis in this manner can be estimated for any value of N , the number of

isolated single poles, and temperature T by evaluating the fourth-order pole term at $x=0$. It can be seen that as the temperature decreases the logarithmic term becomes dominant. The contour of the first integral on the right-hand side of Eq. (A2) can be distorted into the uhp where we know the position of all the poles and branch cut and where

$y_+(z)$ is analytic. We treat the second integral in the lhp likewise. The integral around the branch cut may be reduced to eliminate the logarithm as shown in Ref. 20. There are then two cases of interest; the case where

$$y_+(z) = [y_-(z)]^* \quad (\text{A3})$$

so

$$\left. \frac{\partial y_+(z)}{\partial z} \right|_{z=iP} = \left(\left. \frac{\partial y_-(z)}{\partial z} \right|_{z=-iP} \right)^* \quad (\text{A4})$$

and $y_+(z) + y_-(z) = 2 \operatorname{Re} y_+(z)$ giving the final result

$$\begin{aligned} I = & -2\pi i \frac{kT}{D} \left[\sum_{n=1}^N 2 \operatorname{Re} y_+ \left(i\pi \frac{kT}{D} (2n-1) \right) + \operatorname{Re} y_+(iP) \right] \\ & - i \frac{4\pi^2}{6} \left(\frac{kT}{D} \right)^2 \operatorname{Im} \left(\left. \frac{\partial y_+(z)}{\partial z} \right|_{z=iP} \right) \\ & - 2i \int_P^\infty dx \operatorname{Re} y_+(ix) \end{aligned} \quad (\text{A5})$$

and the case where

$$y_+(z) = -[y_-(z)]^* \quad (\text{A6})$$

so

$$\left. \frac{\partial y_+(z)}{\partial z} \right|_{z=iP} = - \left(\left. \frac{\partial y_-(z)}{\partial z} \right|_{z=-iP} \right)^* \quad (\text{A7})$$

and

$$y_+(z) + y_-(z) = 2i \operatorname{Im} y_+(z) \quad (\text{A8})$$

giving the final result

$$\begin{aligned} I = & 2\pi i \frac{kT}{D} \left[\sum_{n=1}^N 2i \operatorname{Im} y_+ \left(i\pi \frac{kT}{D} (2n-1) \right) + i \operatorname{Im} y_+(iP) \right] \\ & - \frac{4\pi^2}{6} \left(\frac{kT}{D} \right)^2 \operatorname{Re} \left(\left. \frac{\partial y_+(z)}{\partial z} \right|_{z=iP} \right) + 2 \int_P^\infty dx \operatorname{Im} y_+(ix). \end{aligned} \quad (\text{A9})$$

The integrals in Eqs. (A5) and (A9) were separated into three integration regions. The first, being from the point P to a point corresponding to an energy several bandwidths farther along the axis, is mapped to an interval -1 to 1 by a logarithmic mapping and then the integral represented by Gaussian quadrature. This logarithmically mapped region is to provide a distribution of points that join smoothly onto the isolated points even at low temperatures. The second region, from the end

of the first region to a point corresponding to several factors of 10 times the bandwidth, is mapped linearly to -1 to 1 and again Gaussian quadrature is used. The third region, from the end of the second to ∞ , is done by Laguerre quadrature.

The integrals to be evaluated using the above considerations are $\Phi_{g,E}^\sigma(z)$, $\Phi_{g,E}^\sigma(z - \sigma(g_i\gamma + J\Delta/2N))$, $\Phi_{g,E}^\sigma(z - \sigma g_e\gamma)$, their first derivatives at $z=iP$, the special points $\Phi^\sigma(iD - \frac{1}{2}\sigma g_e\gamma)$ and a derivative term χ^σ used to avoid the indeterminacy in the expressions for G_1 , G_2 , etc. For example, see Eq. (62), when $z \rightarrow \frac{1}{2}\sigma g_e\gamma - iD$, we obtain a term

$$F_-^\sigma(z) (\Phi_{+,c}^\sigma(iD - \frac{1}{2}\sigma g_e\gamma) - \Phi_{+,c}^\sigma(z)) - \chi^\sigma,$$

which is treated as another function to be evaluated self-consistently. The process of evaluating the above functions is started by inserting their zero-field values determined from the exact solution to the resultant Riemann-Hilbert boundary value problem.²⁴ Then the process is iterated until convergence for a finite but small external field. These results are used as a starting point for a higher-field calculation, etc. In this way we can obtain results for arbitrary fields and temperatures. The quantities of physical interest are calculated at the same time after convergence is obtained at each field value. The error after each iteration was calculated as the sum of the squares of all relative errors in the functions enumerated above. When this error was less than 10^{-5} , then $\langle S^z \rangle$ was compared with its value at the last iteration. When the error in $\langle S^z \rangle$ was less than 0.0005, the process was considered to have converged and the quantities of physical interest then calculated.

The above procedure was carried out for $T = 1, 5, 10, 30, 70,$ and 100°K and for magnetic fields up to 150 kG ; the results are presented in the figures contained in the text. The number of isolated pole points chosen was such as to represent the Fermi function to eight place accuracy. The number of integral quadrature points used varied with the temperature and field and was as high as 80 for $T = 5^\circ\text{K}$. At temperatures below 5°K and fields above 2 kG the convergence time becomes very long and puts a practical limit to the extent of our calculations as indicated in our results. Also we were constrained to simple iteration by machine memory limitations. See also the remarks in Sec. IIIB.

*Present address: Dept. of Physics, The City College of the City University of New York, N. Y. 10031.

†Present address: Bartram Public High School, Philadelphia, Pa. 19142.

‡Partially supported by Advanced Research Projects Agency.

¹J. Kondo, Progr. Theoret. Phys. (Kyoto) **32**, 37 (1964).

²H. Suhl, Phys. Rev. **138**, A515 (1965); A. A. Abrikosov, Physics **3**, 5 (1965).

³Y. Nagaoka, Phys. Rev. **138**, A1112 (1965); J. Phys. Chem. Solids **27**, 1391 (1966); Progr. Theoret. Phys. (Kyoto) **37**, 13 (1966).

⁴D. N. Zubarev, Usp. Fiz. Nauk. **71**, 71 (1960) [Soviet Phys. Usp. **3**, 320 (1960)].

⁵M. D. Daybell and W. A. Steyert, Rev. Mod. Phys.

- 40, 380 (1968).
- ⁶M. S. Fullenbaum and D. S. Falk, Phys. Rev. 178, 763 (1969).
- ⁷J. Appelbaum and J. Kondo, Phys. Rev. Letters 18, 485 (1967); Phys. Rev. 170, 542 (1968).
- ⁸D. R. Hamann, Phys. Rev. 158, 570 (1967).
- ⁹P. E. Bloomfield and D. R. Hamann, Phys. Rev. 164, 856 (1967).
- ¹⁰A. J. Heeger, L. B. Welsh, M. A. Jensen, and B. Gladstone, Phys. Rev. 172, 302 (1968); A. Narath, A. C. Gossard, and J. H. Wernick, Phys. Rev. Letters 20, 198 (1968).
- ¹¹D. C. Golibersuch and A. J. Heeger, Phys. Rev. 182, 584 (1969).
- ¹²M. S. Fullenbaum and D. S. Falk, Phys. Rev. 157, 452 (1967).
- ¹³M. A. Ruderman and C. Kittel, Phys. Rev. 96, 99 (1954); K. Yosida, *ibid.* 106, 893 (1957).
- ¹⁴H. V. Everts and B. N. Ganguly, Phys. Rev. 174, 594 (1968).
- ¹⁵M. T. Beal-Monod and R. A. Weiner, Phys. Rev. 170, 552 (1968).
- ¹⁶P. Monod, Phys. Rev. Letters 19, 1113 (1967).
- ¹⁷R. More and H. Suhl, Phys. Rev. Letters 20, 500 (1968); R. More, Ph.D. thesis, San Diego, 1968 (unpublished).
- ¹⁸A. P. Klein, Phys. Rev. 172, 520 (1968); 181, 579 (1969).
- ¹⁹F. Takano and T. Ogawa, Progr. Theoret. Phys. (Kyoto) 35, 343 (1966).
- ²⁰P. E. Bloomfield and P. R. Sievert, Phys. Letters 29A, 447 (1969).
- ²¹R. Kubo, J. Phys. Soc. Japan 17, 1100 (1962).
- ²² $(-1)^p (p-1)!$, where p is the number of factors appearing in the factored term. In Eq. (6) $p=2$ for all the terms, excepting the one in Eq. (6d) where $p=3$.
- ²³*Handbook of Mathematical Functions*, edited by M. Abramowitz and I. A. Stegun (U. S. GPO, Washington, D. C., 1964).
- ²⁴P. E. Bloomfield (unpublished); J. Zittartz and E. Müller-Hartmann, Z. Physik 212, 380 (1968).
- ²⁵Preliminary version of our calculations was presented in J. Appl. Phys. 40, 1101 (1969).
- ²⁶This is a simple generalization of the formula of D. R. Hamann (Ref. 8).
- ²⁷S. D. Silverstein and C. B. Duke, Phys. Rev. Letters 18, 695 (1967); Phys. Rev. 161, 462 (1967).
- ²⁸H. Ishii, Progr. Theoret. Phys. (Kyoto) 43, 578 (1970).
- ²⁹R. More (private communication).
- ³⁰J. Zittartz, Z. Physik 217, 155 (1968).
- ³¹A. Narath, K. Brog, and W. Jones, Jr. (unpublished).
- ³²C. Stassis and C. G. Shull, J. Appl. Phys. 41, 1146 (1969).
- ³³A. Narath and A. C. Gossard, Phys. Rev. 183, 391 (1969).
- ³⁴M. D. Daybell and W. A. Steyert, Phys. Rev. 167, 536 (1968).
- ³⁵Y. Osaka, Progr. Theoret. Phys. (Kyoto) 42, 734 (1969).
- ³⁶J. Zittartz, Z. Physik 217, 43 (1968).
- ³⁷C. S. Shastry and B. N. Ganguly, Phys. Letters 29A, 433 (1969).
- ³⁸D. C. Golibersuch, Ph.D. thesis, University of Pennsylvania, 1969 (unpublished); D. C. Golibersuch and A. Heeger (unpublished).
- ³⁹O. J. Lumpkin, Phys. Rev. 164, 324 (1967).
- ⁴⁰N. Rivier and M. J. Zuckerman, Phys. Rev. Letters 21, 904 (1968).
- ⁴¹H. Rohrer, Phys. Rev. 174, 583 (1968).

Static Correlation Function in Dilute Alloys*

B. N. Ganguly

Solid State Division, Oak Ridge National Laboratory, Oak Ridge, Tennessee 37830

and

C. S. Shastry

Department of Physics, Louisiana State University, Baton Rouge, Louisiana 70803

(Received 2 March 1970)

The nonperturbative expression for the static correlation function, $\langle \vec{S}^{e1}(r) \cdot \vec{S}^{imp} \rangle$, formulated in an earlier publication, is computed numerically. Our calculation shows that for large distances ($k_F^{-1} < r < D/T_K$) the static correlation function damps down much faster than $1/r^2$. This is in disagreement with the large-distance $-|a| [(sink_F r)/k_F r]^2$ behavior predicted by some recent calculations.

I. INTRODUCTION

The static correlation function (henceforth referred to as SCF) in dilute magnetic alloys has been subjected to extensive theoretical investigation in the last few years.¹⁻⁶ The SCF is of considerable physical importance, as a spatial average of this

function describes the impurity contribution to the magnetic susceptibility in dilute alloys. In a recent publication, Fullenbaum and Falk³ have examined the SCF on the basis of Nagaoka's theory⁷ as well as the singlet-state theories due to Heeger and Jensen⁸ and Applebaum and Kondo.⁹ They found that for low temperatures the dominant behavior of